Parental age effects and the evolution of senescence

Authors: Patrick M. Barks*, Robert A. Laird

Affiliation:

Department of Biological Sciences

University of Lethbridge

Lethbridge, Alberta, T1K 3M4, Canada

***Corresponding author:** Email: patrick.barks@gmail.com

Running title: Parental age effects shape patterns of senescence

Keywords: senescence, ageing, parental age effect, maternal effect, demography, matrix population models

MS type: Article

ABSTRACT

Most theory on the evolution of senescence implicitly assumes that all offspring are of equal quality. However, in addition to age-related declines in survival and fecundity (classically-defined senescence), many organisms exhibit age-related declines in offspring quality, a phenomenon known as a parental age effect. Theoretical work suggests that parental age effects may alter age-trajectories of selection and therefore shape the evolution of senescence; however, to date, these analyses have been limited to idealized life cycles, and models of maternal care in human populations. To gain a broader understanding of how parental age effects may shape age-trajectories of selection, we extend the classic age-structured population projection model to also account for parental age structure, and apply this model to empirical data from an aquatic plant known to exhibit parental age effects (the duckweed *Lemna minor*), as well as a diverse set of simulated life cycles. Our results suggest that parental age effects alter predictions from classic theory on the evolution of senescence. Age-related declines in offspring quality reduce the relative value of late-life reproduction, leading to steeper age-related declines in the force of natural selection than would otherwise be expected, and potentially favoring the evolution of more rapid rates of senescence.

Introduction

Senescence, an age-related decline in rates of survival and reproduction, seems on its face to be maladaptive, and yet is common across the tree of life (e.g. Aguilaniu et al. 2003, Lindner et al. 2008, Roach et al. 2009, Bouwhuis et al. 2012). Modern evolutionary theory suggests that senescence is ultimately a consequence of a decline in the force of natural selection with increasing age (Hamilton 1966). This decline occurs primarily because, in stable or growing populations, there is a progressive decline in the proportion of individuals occupying increasingly older age classes (Wensink et al. 2017). Intuitively, there is relatively little cost to a mutation that adversely affects an old age class that few individuals occupy, relative to a mutation similarly affecting some younger age class that a greater proportion of mutation carriers will attain. Though more recent analyses suggest that age-related declines in the force of selection are not as inevitable as originally proposed (Vaupel et al. 2004; Baudisch 2005; Caswell and Salguero-Gómez 2013), Hamilton's framework was foundational to the field, and continues to guide evolutionary theory on senescence (reviewed in Rose et al. 2007).

In Hamilton's work, and most subsequent theory on the evolution of senescence (e.g. Abrams 1993, Pedersen 1995, Sozou and Seymour 2004, Baudisch 2005), there is an implicit, simplifying assumption that all offspring are of equal quality (in terms of their lifelong prospects of survival and reproduction), so that fitness depends only on average age-trajectories of survival and fecundity. More precisely, it is typically assumed that survival and fecundity vary only with age, but not with parental age (see section 1 of the supplementary material for an illustration of this distinction). Relaxing this assumption is important for two reasons. First, there is evidence that survival and fecundity do in fact vary with parental age in some taxa (Priest et al. 2002; Descamps et al. 2008; Bouwhuis et al. 2010; Gillespie et al. 2013a; Barks and Laird 2015). Such changes may be due, for example, to the transmission of epigenetic factors from ageing parents to their offspring (Schroeder et al. 2015), age-related changes in parental care or provisioning (Limmer and Becker 2009), or changes in the environment in which offspring develop (Brown and Shine 2009). Thus, the implicit assumption that all offspring are of equal quality does not always hold. Second, recent theoretical results suggest that, if offspring survival or fecundity does decline with increasing parental age, classic methods that ignore such declines may underestimate age-related declines in the force of natural selection (Pavard et al. 2007a,b; Pavard and Branger 2012; Gillespie et al. 2013b). Just as there is little value, for example, in a mutation that increases fecundity within an advanced age class that few individuals occupy, intuitively, there is relatively little value in a mutation that increases fecundity within an age class that inevitably produces offspring with low fitness prospects. This is not to say that parental age effects must themselves be inevitable, but simply that, where they do occur, parental age effects may influence the force of natural selection on age-specific traits.

To our knowledge, the above-cited works (Pavard et al. 2007a,b; Pavard and Branger 2012; Gillespie et al. 2013b), and recent work by Moorad and Nussey (2016), are the only studies to date to examine parental age effects in the context of evolutionary theory on senescence. Pavard et al. modeled a scenario where increasing maternal age increases the probability that offspring become orphaned, where orphans have a reduced chance of surviving to maturity compared to non-orphans. When Pavard et al. applied this model to data from human populations, the maternal age effect resulted in an increased overall force of selection on maternal survival, and a steeper age-related decline in the force of selection on maternal fecundity, compared to what was expected in the absence of the maternal age effect (Pavard et al. 2007a,b; Pavard and Branger 2012). Gillespie et al. modeled a hypothetical population with two age classes and two birth orders (i.e. first-born vs. second-born), where offspring of different birth orders varied in their probability of being born into a 'good environment' and therefore having relatively high lifetime fecundity (compared to offspring born into a 'bad environment'). When second-born offspring had a lower probability of entering the good environment than first-borns, there was a relatively steeper age-related decline in the force of selection than when the two birth orders were equal (Gillespie et al. 2013b). Most recently, Moorad and Nussey (2016) used quantitative genetic approaches to show that age-trajectories of selection on fecundity and offspring quality are likely to differ, and that parental age effects may evolve even in the absence of classically defined senescence in survival or fecundity.

Here we generalize the models of Pavard and colleagues to more broadly test the hypothesis that parental-age-related variation in survival and fecundity alters trajectories of selection on age-specific traits. Specifically, whereas Pavard and colleagues investigated the impact of maternal care on offspring survival to maturity, we construct a model that allows for parental age effects on offspring survival and fecundity, over all possible offspring age classes. We then apply this model to empirical data from an organism known to exhibit negative parental age effects (the aquatic plant *Lemna minor*), as well as simulated life cycles reflecting a continuum of parental age effects, from strongly negative to strongly positive. Our models predict that negative parental age effects (declines in survival or fecundity with increasing parental age) should lead to steeper declines in the force of natural selection than would otherwise be expected, whereas positive parental age effects should have the opposite effect. In extreme cases, positive parental age effects can completely reverse the age-related decline in the force of natural selection on fecundity that is predicted by classic evolutionary theory.

Methods

Overview

Our modeling approach builds on that of Pavard and colleagues (Pavard et al. 2007a,b; Pavard and Branger 2012). We first develop a population projection model structured both by age and parental age (denoted $\boldsymbol{A}^{\mathrm{par}}$), where parental age is the age of a focal individual's parent when the focal individual is born. We then derive a reference projection model ($\boldsymbol{A}^{\mathrm{ref}}$) that lacks parental age structure, but otherwise has similar equilibrium properties to $\boldsymbol{A}^{\mathrm{par}}$ (i.e. the two models have the same finite rate of increase, λ, and stable age distribution). From each model we derive sensitivities of λ to *age*-specific vital rates (i.e. an estimate of the force of natural selection; Hamilton 1966), and then compare age trajectories of these sensitivities between the two models. To gain insight into *why* sensitivities may differ between the two models, we also compare their age-specific reproductive values, which describe the present value of the future offspring of individuals of a given age class (Fisher 1930), or equivalently, the asymptotic contribution of each age class to the population of the distant future (Bienvenu et al. 2017).

For simplicity, our models only track parental age with respect to one parent (i.e. the mother, or the sole parent in an asexual population). Also, our models assume that parental age effects do not compound over multiple generations (e.g. there is no grandparental age effect), which is empirically justified at least in the case of *Lemna* spp. (Barks and Laird 2016). Finally, our models do not account for covariation among vital rates or tradeoffs between parent and offspring traits.

Background: projection of an age-structured population

A simple starting point for demographic analysis is the life cycle graph, which depicts the possible transitions between age classes (and/or stage classes) within a population over one time interval (fig. 1a). In a simple, age-structured population, transitions reflect either survival to the next age class, or reproduction, which always produces individuals of the youngest age class. An age-structured population can be projected through time (Leslie 1945) according to

$$\boldsymbol{n}_{t+1} = \boldsymbol{A}\boldsymbol{n}_t, \tag{1}$$

where $\boldsymbol{n}_t$ is a population vector reflecting the number of individuals in each age class i (from 1 through the maximum attainable age class ω) at time t, and $\boldsymbol{A}$ is a $\omega \times \omega$ projection matrix with per-capita fecundities for each age class across the top row, survival probabilities for age classes 1 through $\omega-1$ on the subdiagonal, and all other elements set to zero, as in

$$\boldsymbol{A} = \begin{pmatrix} F_1 & F_2 & F_3 & \cdots & F_\omega \\ P_1 & 0 & 0 & \cdots & 0 \\ 0 & P_2 & 0 & \cdots & 0 \\ \vdots & \vdots & \ddots & \ddots & \vdots \\ 0 & 0 & \dots & P_{\omega-1} & 0 \end{pmatrix}. \tag{2}$$

(We review some additional aspects of population projection in section 2 of the supplementary material). If transition rates are estimated using a pre-breeding census design (Caswell 2001, Section 2.4.2), fecundity transitions are a product of the birth rate and first-year survival, in which case parental age effects on first-year offspring can be modeled by allowing first-year survival to vary with age. However, this approach does not account for possible parental age effects on offspring survival beyond the first year, or parental age effects on offspring fecundity. We want a model that is able to account for *lifelong* parental age effects.

Incorporating parental age effects

Our first goal is to extend the age-structured life cycle graph in fig. 1a to a graph that accounts for both age and parental age structure (see example in fig. 1b). In this new, multi-trait life cycle, transition rates ($P_{i,j}$ and $F_{i,j}$) depend not just on age class (i), but also parental age class (j). Transitions based on survival increase the age class by 1 but do not affect the parental age class, which is fixed at birth and constant throughout an individual's life. Fecundity, on the other hand, always produces individuals in the youngest age class, but the parental age class transitioned *to* depends on the age class transitioned *from* (i.e. the parental age class of the offspring depends on the age class of the parent). In the example within fig. 1b, the number of parental age classes is equal to the number of age classes, such that an individual within age class i produces offspring with parental age class $j = i$. This correspondence between age classes and parental age classes is convenient, but not necessarily required (either biologically or mathematically). We could, for example, imagine that offspring quality is unaffected by parental age until very late in a parent's life, at which point offspring quality declines. In this case, we might prefer to group some of the early age classes together into one parental age class.

Generalizing to ω age classes and s parental age classes

The population vector $\boldsymbol{n}_t$ now describes a population structured both by age and parental age. It can be written in terms of 'blocks' or sub-vectors, as in

$$\boldsymbol{n}_t = \begin{pmatrix} \boldsymbol{n}_{\text{age}=1} \\ \hline \boldsymbol{n}_{\text{age}=2} \\ \hline \vdots \\ \hline \boldsymbol{n}_{\text{age}=\omega} \end{pmatrix}_t = \begin{pmatrix} n_{1,1} \\ \vdots \\ n_{1,s} \\ \hline n_{2,1} \\ \vdots \\ n_{2,s} \\ \hline \vdots \\ \hline n_{\omega,1} \\ \vdots \\ n_{\omega,s} \end{pmatrix}_t , \tag{3}$$

where $n_{i,j,t}$ is the number of individuals in age class *i* and parental age class *j* at time *t*, *ω* is the maximum attainable age class, and *s* the maximum attainable parental age class ($s \leq \omega$). Here, we have chosen to block the population vector (and corresponding projection matrix) by age class as opposed to parental age class, but this decision is arbitrary and simply requires consistency.

To project the population vector $\boldsymbol{n}_t$ through time we construct a projection matrix $\boldsymbol{A}^{\text{par}}$ reflecting the same age and parental age structure as $\boldsymbol{n}_t$. Specifically, $\boldsymbol{A}^{\text{par}}$ is composed of blocks or submatrices denoted $\boldsymbol{U}_i$ and $\boldsymbol{M}_i$ (of dimension $s \times s$), which give transition probabilities from age class *i* based on survival and fecundity, respectively. Blocks for survival ($\boldsymbol{U}_i$) are arranged on the subdiagonal and blocks for fecundity ($\boldsymbol{M}_i$) across the top row, and all other blocks are $s \times s$ zero matrices ($\boldsymbol{0}$), as in

$$\boldsymbol{A}^{\text{par}} = \begin{pmatrix} \boldsymbol{M}_1 & \boldsymbol{M}_2 & \boldsymbol{M}_3 & \cdots & \boldsymbol{M}_\omega \\ \boldsymbol{U}_1 & \boldsymbol{0} & \boldsymbol{0} & \cdots & \boldsymbol{0} \\ \boldsymbol{0} & \boldsymbol{U}_2 & \boldsymbol{0} & \cdots & \boldsymbol{0} \\ \vdots & \vdots & \ddots & \ddots & \vdots \\ \boldsymbol{0} & \boldsymbol{0} & \cdots & \boldsymbol{U}_{\omega-1} & \boldsymbol{0} \end{pmatrix}. \tag{4}$$

Here we describe the structure of $\boldsymbol{U}_i$ and $\boldsymbol{M}_i$ for the case where age classes and parental age classes correspond exactly ($s = \omega$); see supplementary material section 3 for the $s < \omega$ case. The elements within $\boldsymbol{U}_i$ and $\boldsymbol{M}_i$ are $U_i(k, j)$ and $M_i(k, j)$, respectively, which reflect the probability of a transition from parental age class j to parental age class k, for a given age class i. We note that the new row index k (the parental age class transitioned to) is necessary for specifying $\boldsymbol{A}^{\text{par}}$ because the age- and parental-age indices (i, j) only reflect states being transitioned *from*. Recall that transitions based on survival do not alter the parental age class (which is fixed at birth), so only the diagonal elements of $\boldsymbol{U}_i$ (for which $k = j$) are nonzero, as in

$$\boldsymbol{U_i} = \begin{pmatrix} P_{i,1} & 0 & \cdots & 0 \\ 0 & P_{i,2} & \cdots & 0 \\ \vdots & \vdots & \ddots & \vdots \\ 0 & 0 & \cdots & P_{i,s} \end{pmatrix}. \tag{5}$$

More generally, we map values $U_i(k, j)$ to age-by-parental-age specific survival rates ($P_{i,j}$) based on the formula

$$U_i(k,j) = \begin{cases} P_{i,j}, & \text{if } k = j \\ 0, & \text{else} \end{cases}. \tag{6}$$

For transitions based on fecundity, the parental age class transitioned to (k) depends on the age class transitioned from (i), but is independent of the parental age class transitioned from (j). The block matrices $\boldsymbol{M}_i$ are therefore constructed as follows,

$$\begin{gathered} \boldsymbol{M_1} = \begin{pmatrix} F_{1,1} & F_{1,2} & \cdots & F_{1,s} \\ 0 & 0 & \cdots & 0 \\ \vdots & \vdots & \ddots & \vdots \\ 0 & 0 & \cdots & 0 \end{pmatrix}, \\ \boldsymbol{M_2} = \begin{pmatrix} 0 & 0 & \cdots & 0 \\ F_{2,1} & F_{2,2} & \cdots & F_{2,s} \\ \vdots & \vdots & \ddots & \vdots \\ 0 & 0 & \cdots & 0 \end{pmatrix}, \end{gathered} \tag{7}$$

$$\vdots$$

$$\boldsymbol{M_s} = \begin{pmatrix} 0 & 0 & \cdots & 0 \\ 0 & 0 & \cdots & 0 \\ \vdots & \vdots & \ddots & \vdots \\ F_{s,1} & F_{s,2} & \cdots & F_{s,s} \end{pmatrix}.$$

More generally, values $M_i(k,j)$ are zero except where $k = i$ (i.e. where the age class transitioned from (i) corresponds to the parental age class transitioned to (k)), in which case $M_i(k,j)$ is the per-capita fecundity for an individual in age class i and parental age class j (the parental age class transitioned from), or

$$M_i(k,j) = \begin{cases} F_{i,j}, & \text{if } k = i \\ 0, & \text{else} \end{cases}. \tag{8}$$

We note that the model described above assumes that age-by-parental-age-specific transition rates ($P_{i,j}$ and $F_{i,j}$) have already been estimated, and so is agnostic to their method of estimation (e.g. pre-breeding vs. post-breeding census).

Analysis of age-by-parental-age projection matrix $\boldsymbol{A}^{\text{par}}$

Despite its unique construction from submatrices reflecting different age classes, $\boldsymbol{A}^{\text{par}}$ is fundamentally a multi-trait projection matrix that can be analyzed using standard methods (e.g. Caswell 2001). However, the stable distribution ($\boldsymbol{w}$), reproductive value distribution ($\boldsymbol{v}$), and sensitivities of λ now reflect age-by-parental-age classes, whereas, to facilitate comparison with a reference model lacking parental age structure, we wish to derive the stable *age* distribution ($\widetilde{\boldsymbol{w}}$), *age*-specific reproductive values ($\widetilde{\boldsymbol{v}}$), and sensitivities of λ to *age*-specific vital rates.

Deriving the stable age distribution from the stable age-by-parental-age distribution is straightforward. The relative abundance of age class i at equilibrium ($\widetilde{w}_i$) is simply the sum of the relative age-by-parental-age abundances for that age class over all parental age classes, or

$$\tilde{w}_i = \sum_{j=1}^{s} w_{i,j}. \tag{9}$$

We derive age-specific relative reproductive values ($\tilde{v}_i$) (Bienvenu et al. 2017, Eq. 20) from $\boldsymbol{A}^{\text{par}}$ by averaging across parental age classes weighted by the stable distribution, as in

$$\tilde{v}_i = \frac{\sum_j w_{i,j} v_{i,j}}{\sum_j w_{i,j}}. \tag{10}$$

For the sake of comparison with the reference model, we then scale relative reproductive values such that $\tilde{v}_1 = 1$.

To derive sensitivities of λ^{par} to *age*-specific vital rates, we take the total derivative of λ (Caswell 2001, Eq. 9.36) with respect to the vector of transition rates (either $\boldsymbol{P}_i$ or $\boldsymbol{F}_i$) corresponding to a given age class (i.e. over all parental age classes). For instance, the total derivative of λ with respect to survival at age 1 ($\boldsymbol{P}_1$) is

$$d\lambda = \sum_{j=1}^{s} \frac{\partial \lambda}{\partial P_{1,j}} dP_{1,j}. \tag{11}$$

Age-specific sensitivities derived from $\boldsymbol{A}^{\text{par}}$ in this manner can be understood as the change in λ expected to result from a hypothetical mutation that affects an age-specific vital rate for all members of the given age class, regardless of their parental age class.

Reference model

To understand the evolutionary consequences of parental age effects, we compare age-specific sensitivities derived from $\boldsymbol{A}^{\text{par}}$ to those derived from a reference model ($\boldsymbol{A}^{\text{ref}}$) that lacks parental age structure (i.e. transition rates depend only on age), but is otherwise similar. Specifically, we use the matrix-collapsing algorithm described by Hooley (2000) (see also Salguero-Gómez and Plotkin 2010; Bienvenu et al. 2017; and Coste et al. 2017) to 'collapse' the parental age classes of $\boldsymbol{A}^{\text{par}}$ to yield a standard, age-classified reference matrix (dimensions $\omega \times \omega$) with survival probabilities on the subdiagonal and per-capita fecundities across the top row, as in

$$\boldsymbol{A}^{\text{ref}} = \begin{pmatrix} \tilde{F}_1 & \tilde{F}_2 & \tilde{F}_3 & \cdots & \tilde{F}_\omega \\ \tilde{P}_1 & 0 & 0 & \cdots & 0 \\ 0 & \tilde{P}_2 & 0 & \cdots & 0 \\ \vdots & \vdots & \ddots & \ddots & \vdots \\ 0 & 0 & \ldots & \tilde{P}_{\omega-1} & 0 \end{pmatrix}. \tag{12}$$

Transition rates in the reference model ($\tilde{P}_i$ and $\tilde{F}_i$) are obtained by averaging age-by-parental-age-specific vital rates ($P_{i,j}$ or $F_{i,j}$) across parental age classes within age classes, weighted by the relative proportion of parental age class *j* comprising age class *i* at the stable distribution, or

$$\tilde{P}_i = \frac{1}{\tilde{w}_i} \sum_{j=1}^{s} P_{i,j} w_{i,j}, \tag{13}$$

$$\tilde{F}_i = \frac{1}{\tilde{w}_i} \sum_{j=1}^{s} F_{i,j} w_{i,j}. \tag{14}$$

As shown by Hooley (2000) (see also Bienvenu et al. 2017 and Coste et al. 2017), this method of collapsing a projection matrix to a smaller dimension preserves λ and the relative stable distribution, but does not generally preserve the relative reproductive value distribution or sensitivities of λ (we discuss alternative collapsing methods in section 4 of the supplementary material).

Once $\boldsymbol{A}^{\text{ref}}$ has been populated with the transition rates described above, we use standard techniques (described in supplementary material section 2) to determine the sensitivity of λ^{ref} to $\tilde{P}_i$ and $\tilde{F}_i$.

Comparing selection gradients between $\boldsymbol{A}^{\mathrm{par}}$ and $\boldsymbol{A}^{\mathrm{ref}}$

Our approach requires a comparison of the relative 'steepness' (i.e. slope) of age-specific sensitivity trajectories. If these trajectories were always linear (or could be transformed to linearity) then it would be straightforward to compare their slopes. However, in practice, sensitivity trajectories derived from realistic life cycles are not always linear. In the current analysis, we use a simple heuristic to compare slopes of sensitivity trajectories, which is valid for almost all of the cases that we examined. Specifically, if two age-trajectories **x** and **y** are each monotonic, and at the lowest age class the value of **x** is greater than **y** ($x_1 > y_1$), while at the maximum age class the value of **x** is lower than **y** ($x_\omega < y_\omega$), then the slope of trajectory **x** must be steeper (i.e. numerically lower) than the slope of **y**. In two cases that we examined (based on simulated life cycles, described subsequently), sensitivity trajectories from $\boldsymbol{A}^{\mathrm{par}}$ and $\boldsymbol{A}^{\mathrm{ref}}$ never intersected (i.e. sensitivities from one model were higher than sensitivities from the other, at all age classes), rendering our simple heuristic invalid. We discuss these exceptions subsequently.

Construction and analysis of $\boldsymbol{A}^{\mathrm{par}}$ in practice

Our analyses were conducted in R 3.5.1 (R Core Team 2018), and the relevant data and scripts are available on GitHub (https://github.com/patrickbarks/parental-age) and archived at the Dryad Digital Repository (Barks and Laird, 2019). In practice, multi-trait projection models can be constructed and analyzed element-by-element, just like a single-trait model; however, keeping track of which elements correspond to which traits (or which indices to which blocks) can be tedious if the number of groups within each trait is large. To construct and analyze our age-by-parental-age models we adopted the vec-permutation approach of Caswell (2012) (see also Caswell and Salguero-Gómez 2013). In the vec-permutation approach, we construct a series of single-trait matrices representing the separate blocks of $\boldsymbol{A}^{\text{par}}$ ($\boldsymbol{U}_i$ and $\boldsymbol{M}_i$), and then merge those blocks into our final multi-trait projection model using the equations given in Caswell (2012). The vec-permutation approach also simplifies sensitivity analysis on $\boldsymbol{A}^{\text{par}}$ by allowing us to extract sensitivities in blocks reflecting the same structure as $\boldsymbol{U}_i$ and $\boldsymbol{M}_i$. Once $\boldsymbol{A}^{\text{par}}$ has been constructed, we test to ensure ergodicity and irreducibility using the R library POPDEMO (Stott et al. 2012).

Empirical data: parental age effects in Lemna minor

We applied the modeling approach described above to demographic data from a laboratory study on parental age effects in ramets of the aquatic plant *Lemna minor* L. — a tiny aquatic angiosperm with a short lifespan and rapid rate of asexual reproduction (Barks and Laird 2014, 2015). In that study, to understand the effect of parental age on offspring demographic rates, the authors tracked all of the 542 ramet offspring detached from an initial cohort of 41 parental plants (also referred to as ‘fronds’). The offspring — all of known parental age — were cultured in individual Petri dishes within growth chambers, and monitored daily for survival and fecundity over the course of their lives (see section 5 of the supplementary material for details on the census methodology used in that study). For the current study, we combined parental ages (which ranged from 1–29 days) into $s = 8$ parental age categories of similar sample size (using the *quantile* function in R), and obtained smoothed age-by-parental-age specific transition rates ($P_{i,j}$ and $F_{i,j}$) using generalized additive models relating survival (binomial error) or number of offspring released (Poisson error) to plant age (see further details in section 6 of the supplementary material).

Simulated life cycles

To assess the generality of the model results from *L. minor*, we also applied the parental age model to five simulated life cycles (i.e. simulated trajectories of $P_{i,j}$ and $F_{i,j}$) reflecting a continuum of possible parental age effects, from strongly negative to strongly positive. Each life cycle was parameterized with age-independent rates of survival and fecundity and a stasis loop at the maximum modeled age class ($\omega = 20$), so as not to exhibit senescence in the classical sense (i.e. except for the potential parental age effects). The stasis loop is necessary to prevent survival and fecundity from dropping to zero after the maximum modeled age class, and therefore creating an inherently senescent life cycle. For the sake of comparability, transition rates P_j and F_j were adjusted to ensure that $\lambda = 1$ for each life cycle. Further details are given in supplementary material section 7. Note that the five simulated life cycles we examine in the main text exhibit parental age effects only on fecundity, but we also explore parental age effects on survival in supplementary material section 8 (the results are qualitatively similar). In supplementary analyses we also explore the impact of varying λ (i.e. setting it less than or greater than 1; supplementary material section 8).

Finally, we investigated whether classic predictions from evolutionary theory still hold given parental age effects. Specifically, we sought to find a counterexample to Hamilton's prediction that, given a stable or increasing population ($\lambda \geq 1$), sensitivities of λ to survival and fecundity *must* decline with increasing age following reproductive maturity

(Hamilton 1966, Wensink et al. 2017). Because negatively-senescent trajectories of survival and fecundity are expected to yield the slowest age-related declines in the force of natural selection, we constructed a life cycle with strong age-related increases in both survival and fecundity, as well as strongly positive parental age effects on survival and fecundity (with vital rates adjusted to maintain $\lambda = 1$). We then compared selection gradients from a model accounting for the parental age effects to a model ignoring them, as described above.

Results

Empirical parental age effects in Lemna minor

The parental age effect on survival in *L. minor* was relatively weak and inconsistent, except for a slight decline in rates of late-life survival (ages > 20 days) with increasing parental age (fig. 2a). The parental age effect on fecundity was stronger, with plants of high parental age having reduced rates of early-life fecundity (fig. 2b). At older age classes however (ages > 20 days), this pattern reversed, with plants of high parental age having somewhat higher fecundity late in life (fig. 2b).

With respect to the parental age model ($\boldsymbol{A}^{\text{par}}$), the expected proportion of individuals at the stable distribution declined markedly with increasing age and parental age (fig. 2c). At equilibrium, the first three parental age classes (parental age ≤ 8 days) were expected to comprise 97% of the population. The reproductive value distribution generally mirrored the fecundity distribution, declining with age after an early-life peak, and declining with increasing parental age only among early age classes (fig. 2d). Age-specific relative reproductive values from $\boldsymbol{A}^{\text{par}}$ declined more strongly with age than those from $\boldsymbol{A}^{\text{ref}}$ (fig. 3b).

Sensitivities of λ^{par} to survival and fecundity also declined strongly with increasing age and parental age (fig. 2e,f). In line with our prediction, age-specific sensitivities derived from $\boldsymbol{A}^{\text{par}}$ were greater among the youngest age classes and lower among the oldest age classes than corresponding sensitivities derived from $\boldsymbol{A}^{\text{ref}}$ (fig. 3). That is, sensitivities declined more strongly with age when the negative parental age effect was accounted for. However, this effect was small compared to the overall decline in sensitivity with age. For instance, the sensitivity of λ to fecundity at age 1 was only 4% higher when we accounted for parental age effects (i.e. comparing sensitivities from $\boldsymbol{A}^{\text{par}}$ vs. $\boldsymbol{A}^{\text{ref}}$), whereas the sensitivity of λ to fecundity at age 1 was 51% higher than at age 2, regardless of the model.

Simulated life cycles

For the simulated life cycle representing a strongly negative parental age effect on fecundity, the model accounting for parental age effects ($\boldsymbol{A}^{\text{par}}$) yielded sharper age-related declines in sensitivities of λ to survival and fecundity than the model that ignored the parental age effect ($\boldsymbol{A}^{\text{ref}}$) (fig. 4, leftmost column). In contrast, for the life cycle representing a strongly positive parental age effect on fecundity, the model accounting for parental age effects ($\boldsymbol{A}^{\text{par}}$) yielded shallower age-related declines in sensitivities of λ to survival and fecundity than the reference model ($\boldsymbol{A}^{\text{ref}}$) (fig. 4, rightmost column). As was the case in the analysis on *L. minor*, the impact of parental age effects on sensitivities was small relative to the effect of age.

Patterns in age-specific relative reproductive value were qualitatively similar. Because the simulated life cycles did not exhibit senescence in the classical sense (i.e. survival and fecundity were constant with age), relative reproductive values from the models that ignored parental age effects ($\boldsymbol{A}^{\text{ref}}$) were constant with age (fig. 4). However, accounting for a negative parental age effect led to a decline in relative reproductive value with age, whereas accounting for a positive parental age effect led to an increase in relative reproductive value with age (fig. 4).

We show in section 8 of the supplementary material that the general results described above are robust to a variety of alternative parameterizations, with two possible exceptions. Specifically, for the simulated life cycle with a negative parental age effect on fecundity and a high population growth rate ($\lambda = 1.4$) (supplementary material section 8a), survival sensitivities from $\boldsymbol{A}^{\text{par}}$ were lower than those from $\boldsymbol{A}^{\text{ref}}$ at all age classes. Conversely, for the simulated life cycle with a strongly positive parental age effect on survival (supplementary material section 8b), survival sensitivities from $\boldsymbol{A}^{\text{par}}$ were higher than those from $\boldsymbol{A}^{\text{ref}}$ across all age classes. In both cases, simple linear regressions fit to each sensitivity trajectory (on a semi-log scale, under which trajectories were very close to linear) yielded the expected difference in slope. That is, a negative parental age effect led to a steeper slope for the sensitivity trajectory from $\boldsymbol{A}^{\text{par}}$, and vise versa for the positive parental age effect.

For our simulated life cycle constructed to test the limits of classic evolutionary theory, with strong age- and parental-age-related increases in both survival and fecundity, we found that sensitivities of λ to survival did in fact decline with age even when the parental age effect was accounted for, consistent with Hamilton's prediction (fig. 5). In contrast, sensitivities of λ to fecundity declined with age in the model ignoring the parental age effect, as expected, but progressively increased with age (following a minimum around age 4) in the model accounting for the parental age effect (fig. 5), contrary to Hamilton's prediction.

Discussion

Our results suggest that parental age effects modify predictions from classic evolutionary theory regarding age-specific selection gradients on survival and fecundity. In particular, negative parental age effects (i.e. declines in survival or fecundity with increasing parental age) lead to steeper age-related declines in the force of natural selection than would otherwise be expected, because they lower the relative contribution of late-life reproduction to fitness. Intuitively, if offspring produced late in life tend to have relatively low prospects for survival and reproduction, then the premium on early reproduction will be relatively increased. The opposite is true for positive parental age effects, which lead to increases in the relative value of late-life reproduction, and a shallower decline in the force of selection with age than would be expected in the absence of the parental age effect. In extreme cases, when combined with age-related increases in survival and fecundity, positive parental age effects may even reverse one of the classic predictions of evolutionary theory on senescence — that selection gradients necessarily decline with age when a population is stable or growing (Hamilton 1966). This result is an extreme case of a more general finding from Caswell and Salguero-Gómez (2013), that projection models structured by both age and developmental stage may yield very different age-gradients of selection than models based only on age.

The main results that we describe above are generally consistent with those of Gillespie et al. (2013b), who examined a model with two age classes and two birth orders, where offspring of different birth orders varied in their probability of being born into a 'good environment' and therefore having relatively high lifetime fecundity (compared to offspring born into a 'bad environment'). As in our study, Gillespie et al. found that negative birth order effects led to relatively steeper age-gradients of selection on both survival and fecundity, whereas positive birth order effects led to shallower selection gradients. Because our study builds directly on the work of Gillespie et al., we think it important to highlight the novel contributions of our approach and analyses. First, our analysis confirms that the results of Gillespie et al. hold under a wider variety of modeling assumptions. These include models with (i) more than two parental age classes, (ii) non-monotonic parental age effects, and (iii) parental age effects on survival rather than fecundity. Second, based on both simulated and empirically-parameterized models, our analyses suggest that parental age effects tend to have relatively small impacts on selection gradients (we return to this point in the following paragraph). Finally, our analyses uncovered nuances that can guide future theoretical work. For example, in most of the models we examined, negative parental age effects led to relatively increased sensitivities at the youngest age classes and relatively decreased sensitivities at the oldest age classes, relative to the corresponding reference model. However, in a few cases, parental age effects led to relatively increased (or decreased) sensitivities across *all* age classes. Future theoretical work should examine the conditions under which parental age effects modify the overall force of selection on a given vital rate, independent of age.

Despite one extreme example of a positive parental age effect reversing the age-related selection gradient on fecundity, most of our analyses in fact indicated a relatively small impact of parental age effects on selection gradients. This was despite the fact that the magnitude of the empirical parental age effect that we examined in *L. minor* was quite strong — the maximum fecundity of plants in the youngest parental age group was almost twice as high as those in the oldest parental age group (fig. 2b). Furthermore, the parental age effects that we examined were primarily monotonic (i.e. consistently increasing or declining with age; except for *L. minor* which exhibited a slight reversal of the parental age effect at late age classes), which may not always be the case in nature (e.g. Bouwhuis et al. 2010). For example, among species that exhibit parental care, offspring quality may initially increase with age as parents become more experienced or gain better territories, but later decline as parents senesce. Presumably, the two trends in offspring quality (initially increasing and later declining) would partially balance out, leading to a selection gradient relatively similar to what would be expected in the absence of the parental age effect.

Given the general and flexible framework that we describe, it should be straightforward to examine the impact of parental age effects on selection gradients in any other species for which the requisite data are available (age- and parental-age-specific estimates of survival and fecundity). However, such data can be challenging and time consuming to collect — generally requiring at least two generations of study, and the ability to ascertain parent-offspring relationships. That said, the requisite data are likely already available for many animal populations subject to long-term demographic study, such as Soay sheep (Jones et al. 2005), red deer (Foerster et al. 2007), ground squirrels (Gedir and Michener 2014), and great tits (Bouwhuis et al. 2010).

Apart from a greater availability of empirical data, continuing research on parental age effects will be bolstered by a recent surge in theory relating to multi-trait projection matrices (Caswell 2012; Steiner et al. 2014; Roth and Caswell 2016; Coste et al. 2017). Whereas most projection analyses are based on life cycles structured according to a single variable (sometimes called the *i*-state; usually either age or size), the analysis of parental age effects requires models that track at least two traits — age and parental age. While two-trait projection models are not by any means new, the recent introduction of the 'vec-permutation' framework greatly simplifies the construction and analysis of such models (Caswell 2012; Caswell and Salguero-Gómez 2013). More recently, Coste et al. (2017) have introduced an alternative technique for constructing multi-trait projection models based on sparse matrices, and have also developed a general approach for the analysis of single traits within multi-trait models. This latter approach is analogous (but more general) to the approach used in the current study, where, following Pavard and colleagues (Pavard et al. 2007a,b; Pavard and Branger 2012), we assess age-specific traits in models structured by both age and parental age. The above-described tools will make it easier not only to extend the analyses described here to other taxa, but also to conduct more nuanced analyses that control for other demographically-important traits such as sex, location, and environmental condition.

In the current study, we demonstrate that parental age effects modify selection gradients on age-specific traits — in extreme cases even reversing the direction of the selection gradient predicted by classic evolutionary theory (in the case of fecundity, though not survival). However, the magnitude of this effect was small in the one empirical dataset that we examined (from a laboratory study on the aquatic plant *Lemna minor*), and in most of the simulated life cycles as well. As with all models, ours was a simplification of reality. In particular, we did not consider density-dependence (Abrams 1993), covariation among vital rates (Charlesworth 1990), tradeoffs between parent and offspring traits (Smith and Fretwell 1974), or stochasticity (Tuljapurkar et al. 2009), each of which may influence demographic and evolutionary dynamics. Nonetheless, comparative studies have demonstrated incredible diversity in patterns of senescence across the tree of life (Ricklefs 2010, Baudisch et al. 2013, Jones et al. 2014), much of which remains unexplained by existing evolutionary theory (Williams et al. 2006). Because parental age effects are known to occur in a wide range of taxa, and may modify trajectories of selection on age-specific traits, the further incorporation of parental age effects into evolutionary theory on senescence is an important challenge.

Acknowledgments

We gratefully acknowledge funding from the Natural Sciences and Engineering Research Council of Canada through a Canada Graduate Scholarship to P.M.B. and a Discovery Grant to R.A.L. (Grant no. RGPIN-2015-05486). We thank associate editor Tom Miller and two anonymous reviewers for constructive feedback. The authors declare no conflict of interest.

Author contributions: P.M.B. and R.A.L. conceived the idea for the study, P.M.B. performed the modeling and analyses, and P.M.B. wrote the manuscript with feedback and editing from R.A.L.

Data and code availability: Data and R scripts required to reproduce our analyses are available on GitHub (https://github.com/patrickbarks/parental-age), and archived at the Dryad Digital Repository (https://doi.org/10.5061/dryad.15dv41nt0).

Literature Cited

Abrams, P. A. 1993. Does increased mortality favor the evolution of more rapid senescence? Evolution 47:877–887.

Aguilaniu, H., L. Gustafsson, M. Rigoulet, and T. Nystrom. 2003. Asymmetric inheritance of oxidatively damaged proteins during cytokinesis. Yeast 20:S303–S303.

Barks, P. M., and R. A. Laird. 2014. Data from: Senescence in duckweed: age-related declines in survival, reproduction, and offspring quality. Dryad Digital Repository, https://doi.org/10.5061/dryad.t938n

——. 2015. Senescence in duckweed: age-related declines in survival, reproduction and offspring quality. Functional Ecology 29:540–548.

——. 2016. A multigenerational effect of parental age on offspring size but not fitness in common duckweed (*Lemna minor*). Journal of Evolutionary Biology 29:748–756.

——. 2019. Data from: Parental age effects and the evolution of senescence. American Naturalist, Dryad Dataset, https://doi.org/10.5061/dryad.15dv41nt0

Baudisch, A. 2005. Hamilton's indicators of the force of selection. Proceedings of the National Academy of Sciences of the USA 102:8263–8268.

Baudisch, A., R. Salguero-Gómez, O. R. Jones, T. Wrycza, C. Mbeau-Ache, M. Franco, and F. Colchero. 2013. The pace and shape of senescence in angiosperms. Journal of Ecology 101:596–606.

Bienvenu, F., E. Akcay, S. Legendre, and D. M. McCandlish. 2017. The genealogical decomposition of a matrix population model with applications to the aggregation of stages. Theoretical Population Biology 115:69–80.

Bouwhuis, S., A. Charmantier, S. Verhulst, and B. C. Sheldon. 2010. Trans-generational effects on ageing in a wild bird population. Journal of Evolutionary Biology 23:636–642.

Bouwhuis, S., R. Choquet, B. C. Sheldon, and S. Verhulst. 2012. The forms and fitness cost of senescence: age-specific recapture, survival, reproduction, and reproductive value in a wild bird population. The American Naturalist 179:E15–E27.

Brown, G. P., and R. Shine. 2009. Beyond size–number trade-offs: clutch size as a maternal effect. Philosophical Transactions of the Royal Society B 364:1097–1106.

Caswell, H. 2001. *Matrix population models: construction, analysis, and interpretation, 2nd ed*. Sinauer, Sunderland, MA.

——. 2012. Matrix models and sensitivity analysis of populations classified by age and stage: a vec-permutation matrix approach. Theoretical Ecology 5:403–417.

Caswell, H., and R. Salguero-Gómez. 2013. Age, stage and senescence in plants. Journal of Ecology 101:585–595.

Charlesworth, B. 1990. Optimization models, quantitative genetics, and mutation. Evolution 44:520–538.

Coste, C. F., F. Austerlitz, and S. Pavard. 2017. Trait level analysis of multitrait population projection matrices. Theoretical Population Biology 116:47–58.

Descamps, S., S. Boutin, D. Berteaux, and J. M. Gaillard. 2008. Age-specific variation in survival, reproductive success and offspring quality in red squirrels: evidence of senescence. Oikos 117:1406–1416.

Fisher, R. A. 1930. *The genetical theory of natural selection*. Clarendon Press, Oxford, England.

Foerster, K., T. Coulson, B. C. Sheldon, J. M. Pemberton, T. H. Clutton-Brock, and L. E. Kruuk. 2007. Sexually antagonistic genetic variation for fitness in red deer. Nature 447:1107–1110.

Gedir, J. V., and G. R. Michener. 2014. Litter sex ratios in Richardson's ground squirrels: long-term data support random sex allocation and homeostasis. Oecologia 174:1225–1239.

Gillespie, D. O. S., A. F. Russell, and V. Lummaa. 2013a. The effect of maternal age and reproductive history on offspring survival and lifetime reproduction in preindustrial humans. Evolution 67:1964–1974.

Gillespie, D. O. S., M. V. Trotter, S. Krishna-Kumar, and S. D. Tuljapurkar. 2013b. Birth-order differences can drive natural selection on aging. Evolution 68:886–892.

Hamilton, W. D. 1966. The moulding of senescence by natural selection. Journal of Theoretical Biology 12:12–45.

Hooley, D. E. 2000. Collapsed matrices with (almost) the same eigenstuff. The College Mathematics Journal 31:297–299.

Jones, O. R., M. J. Crawley, J. G. Pilkington, and J. M. Pemberton. 2005. Predictors of early survival in Soay sheep: cohort-, maternal-and individual-level variation. Proceedings of the Royal Society B 272:2619–2625.

Jones, O. R., A. Scheuerlein, R. Salguero-Gómez, C. G. Camarda, R. Schaible, B. B. Casper, J. P. Dahlgren, et al. 2014. Diversity of ageing across the tree of life. Nature 505:169-173.

Kern, S., M. Ackermann, S. C. Stearns, and T. J. Kawecki. 2001. Decline in offspring viability as a manifestation of aging in *Drosophila melanogaster*. Evolution 55:1822–1831.

Leslie, P. H. 1945. On the use of matrices in certain population mathematics. Biometrika 33:183–212.

Limmer, B., and P. H. Becker. 2009. Improvement in chick provisioning with parental experience in a seabird. Animal Behaviour 77:1095–1101.

Lindner, A. B., R. Madden, A. Demarez, E. J. Stewart, and F. Taddei. 2008. Asymmetric segregation of protein aggregates is associated with cellular aging and rejuvenation. Proceedings of the National Academy of Sciences of the USA 105:3076–3081.

Moorad, J. A., and D. H. Nussey. 2016. Evolution of maternal effect senescence. Proceedings of the National Academy of Sciences of the USA 113:362–367.

Pavard, S., and F. Branger. 2012. Effect of maternal and grandmaternal care on population dynamics and human life-history evolution: A matrix projection model. Theoretical Population Biology 82:364–376.

Pavard, S., D. N. Koons, and E. Heyer. 2007a. The influence of maternal care in shaping human survival and fertility. Evolution 61:2801–2810.

Pavard, S., A. Sibert, and E. Heyer. 2007b. The effect of maternal care on child survival: a demographic, genetic, and evolutionary perspective. Evolution 61:1153–1161.

Pedersen, B. 1995. An evolutionary theory of clonal senescence. Theoretical Population Biology 47:292–320.

Priest, N. K., B. Mackowiak, and D. E. L. Promislow. 2002. The role of parental age effects on the evolution of aging. Evolution 56:927–935.

R Core Team. 2018. *R: A language and environment for statistical computing*. R Foundation for Statistical Computing, Vienna, Austria. http://www.R-project.org

Ricklefs, R. E. 2010. Insights from comparative analyses of aging in birds and mammals. Aging Cell 9:273–284.

Roach, D. A., C. Ridley, and J. Dudycha. 2009. Longitudinal analysis of *Plantago*: Age by environment interactions reveal aging. Ecology 90:1427–1433.

Rose, M. R., C. L. Rauser, G. Benford, M. Matos, and L. D. Mueller. 2007. Hamilton's forces of natural selection after forty years. Evolution 61:1265–1276.

Roth, G., and H. Caswell. 2016. Hyperstate matrix models: Extending demographic state spaces to higher dimensions. Methods in Ecology and Evolution 7:1438–1450.

Salguero-Gomez, R., and J. B. Plotkin. 2010. Matrix dimensions bias demographic inferences: implications for comparative plant demography. American Naturalist 176:710–722.

Schroeder, J., S. Nakagawa, M. Rees, M. E. Mannarelli, and T. Burke. 2015. Reduced fitness in progeny from old parents in a natural population. Proceedings of the National Academy of Sciences of the USA 112:4021–4025.

Smith, C. C., and S. D. Fretwell. 1974. The optimal balance between size and number of offspring. American Naturalist 108:499–506.

Sozou, P. D., and R. M. Seymour. 2004. To age or not to age. Proceedings of the Royal Society B 271:457–463.

Steiner, U. K., S. Tuljapurkar, and T. Coulson. 2014. Generation time, net reproductive rate, and growth in stage-age-structured populations. American Naturalist 183:771–783.

Stott, I., D. J. Hodgson, and S. Townley. 2012. popdemo: an R package for population demography using projection matrix analysis. Methods in Ecology and Evolution 3:797–802.

Tuljapurkar, S., J .M. Gaillard, and T. Coulson. 2009. From stochastic environments to life histories and back. Philosophical Transactions of the Royal Society B 364:1499–1509.

Vaupel, J. W., A. Baudisch, M. Dölling, D. A. Roach, and J. Gampe. 2004. The case for negative senescence. Theoretical Population Biology 65:339–351.

Wensink, M. J., H. Caswell, and A. Baudisch. 2017. The rarity of survival to old age does not drive the evolution of senescence. Evolutionary Biology 44:5–10.

Williams, G. C. 1957. Pleiotropy, natural selection, and the evolution of senescence. Evolution 11:398–411.

Williams, P. D., T. Day, F. Quinn, and L. Rowe. 2006. The shaping of senescence in the wild. Trends in Ecology and Evolution 21:458–463.

References Cited Only in the Online Enhancements

Pedersen, E. J., D. L. Miller, G. L. Simpson, and N. Ross. 2019. Hierarchical generalized additive models in ecology: an introduction with mgcv. PeerJ 7:e6876.

Wood, S. N. 2011. Fast stable restricted maximum likelihood and marginal likelihood estimation of semiparametric generalized linear models. Journal of the Royal Statistical Society: Series B 73:3–36.

Figure Legends

Figure 1: Example life cycle diagrams and projection matrices structured only by age (**a**), or by age and parental age (**b**). Red arrows and squares represent survival transitions (P) whereas blue arrows and squares reflect fecundity (F). In (**a**), the life cycle is structured only by age, and so transition rates (P_i and F_i) are indexed only by age class *i*. In (**b**), the life cycle is structured by both age and parental age, so transition rates are indexed by age class *i* and parental age class *j* (note that some fecundity labels, on light blue lines, are omitted to limit clutter).

Figure 2: Equilibrium traits in *Lemna minor* based on a projection model structured by age and parental age ($\boldsymbol{A}^{\text{par}}$; thick green lines), compared to a reference model structured only by age ($\boldsymbol{A}^{\text{ref}}$; dashed line). Values in the left-most column reflect transition rate inputs to the respective models, whereas values in the middle and right columns reflect model outputs (i.e. stable distribution, reproductive value, and sensitivities of λ to vital rates). Note that in (c), the stable weights from $\boldsymbol{A}^{\text{par}}$ (thick green lines) do sum to equal the stable weights from $\boldsymbol{A}^{\text{ref}}$ (dashed line), but this is hard to see because of the line width and log scale. Reproductive values from $\boldsymbol{A}^{\text{par}}$ in (d) are scaled such that $\tilde{v}_1 = 1$, where $\tilde{v}_i$ represents the relative reproductive value for age class *i* as defined in the main text.

Figure 3: Age-specific stable distribution (a), reproductive value (b), and sensitivities of vital rates to selection (c, d) for *Lemna minor* based on a projection model structured by age and parental age ($\boldsymbol{A}^{\text{par}}$; solid line), compared to a reference model structured only by age ($\boldsymbol{A}^{\text{ref}}$; dashed line). Reproductive values from $\boldsymbol{A}^{\text{par}}$ in (b) represent age-specific relative

reproductive values, as defined in the main text. Though not clearly visible, note that at the youngest age class, age-specific sensitivities from $\boldsymbol{A}^{\mathrm{par}}$ (c, d) are slightly higher than the corresponding sensitivities from $\boldsymbol{A}^{\mathrm{ref}}$.

Figure 4: Model inputs and age-specific outputs with respect to five simulated life cycles spanning a continuum of parental age effects, from strongly negative (leftmost column) to strongly positive (rightmost column). The top two rows show transition rate inputs to the respective models (model $\boldsymbol{A}^{\mathrm{par}}$ accounts for parental age effects whereas $\boldsymbol{A}^{\mathrm{ref}}$ does not), whereas the bottom three rows depict age-specific model outputs: relative reproductive values (as defined in the text), sensitivities of λ to survival ($\mathrm{d}\lambda/\mathrm{d}P$), and sensitivities of λ to fecundity ($\mathrm{d}\lambda/\mathrm{d}F$).

Figure 5: Model inputs (top row) and corresponding age-specific sensitivities (bottom row) with respect to a simulated life cycle with strong age- and parental-age-related increases in survival and fecundity. Model $\boldsymbol{A}^{\mathrm{par}}$ accounts for parental age effects whereas $\boldsymbol{A}^{\mathrm{ref}}$ does not.

Figure 1

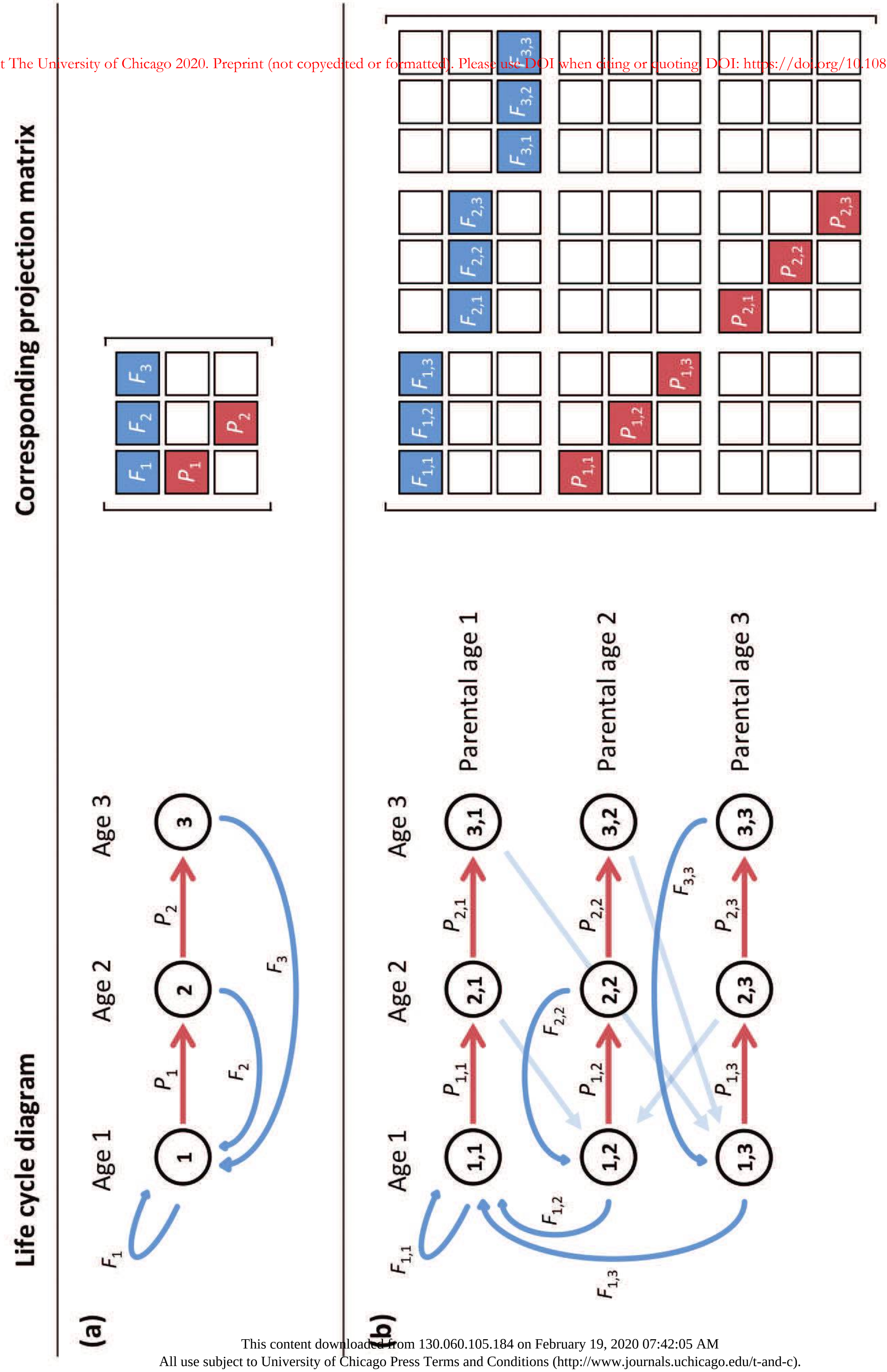
Life cycle diagram
Corresponding projection matrix
(a)
Age 1
Age 2
Age 3
1
2
3
P_1
P_2
F_1
F_2
F_3
F_1 F_2 F_3
P_1
P_2
(b)
Parental age 1
Parental age 2
Parental age 3
1,1
2,1
3,1
1,2
2,2
3,2
1,3
2,3
3,3
$P_{1,1}$
$P_{2,1}$
$P_{1,2}$
$P_{2,2}$
$P_{1,3}$
$P_{2,3}$
$F_{1,1}$
$F_{1,2}$
$F_{1,3}$
$F_{2,2}$
$F_{3,3}$
$F_{1,1}$ $F_{1,2}$ $F_{1,3}$
$F_{2,1}$ $F_{2,2}$ $F_{2,3}$
$F_{3,1}$ $F_{3,2}$ $F_{3,3}$
$P_{1,1}$ $P_{1,2}$ $P_{1,3}$
$P_{2,1}$ $P_{2,2}$ $P_{2,3}$

Figure 2

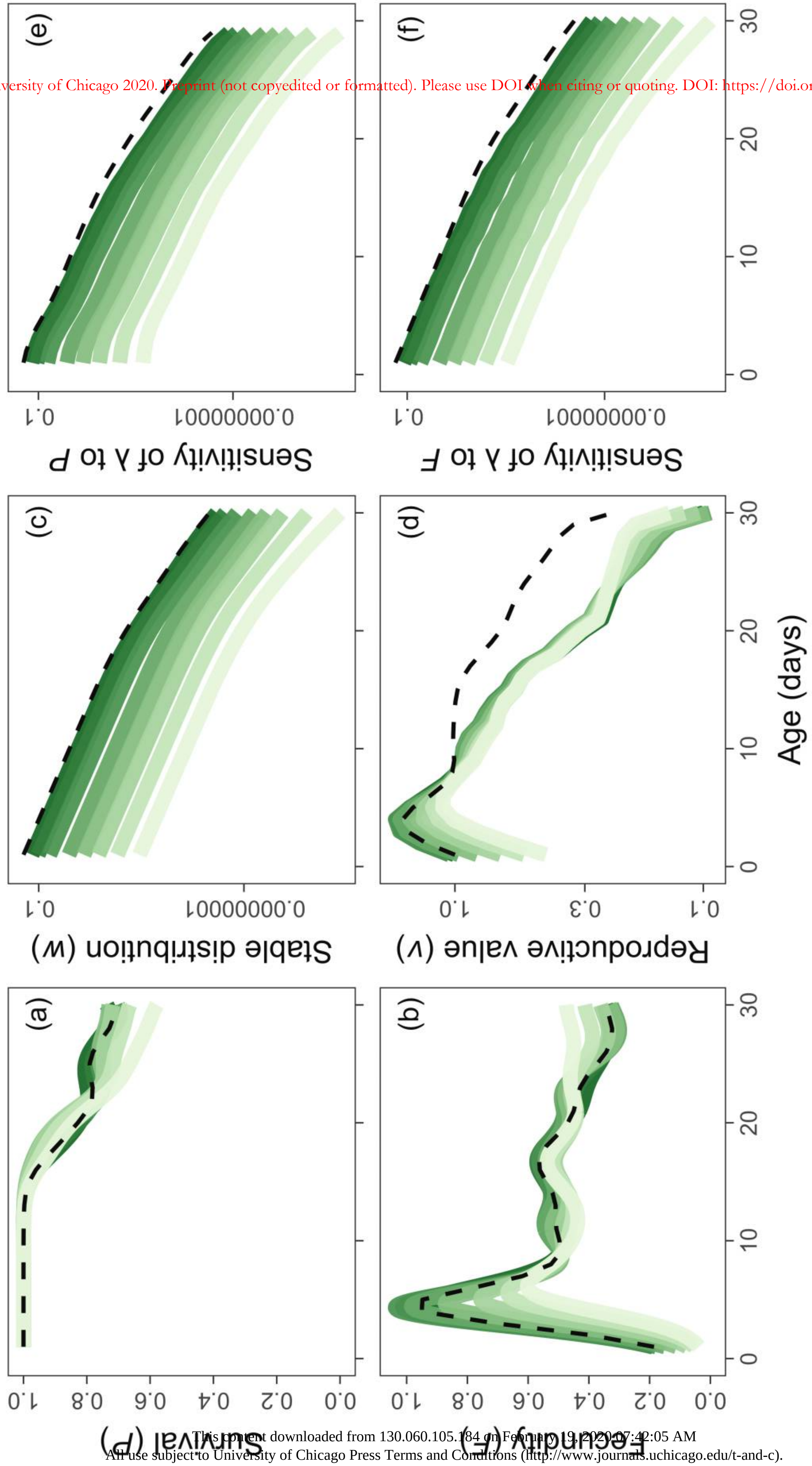
(a)
Survival (P)
1.0
0.8
0.6
0.4
0.2
0.0
(b)
Fecundity (F)
1.0
0.8
0.6
0.4
0.2
0.0
(c)
Stable distribution (w)
0.1
0.00000001
(d)
Reproductive value (v)
1.0
0.3
0.1
(e)
Sensitivity of λ to P
0.1
0.00000001
(f)
Sensitivity of λ to F
0.1
0.00000001
0
10
20
30
Age (days)

Figure 3

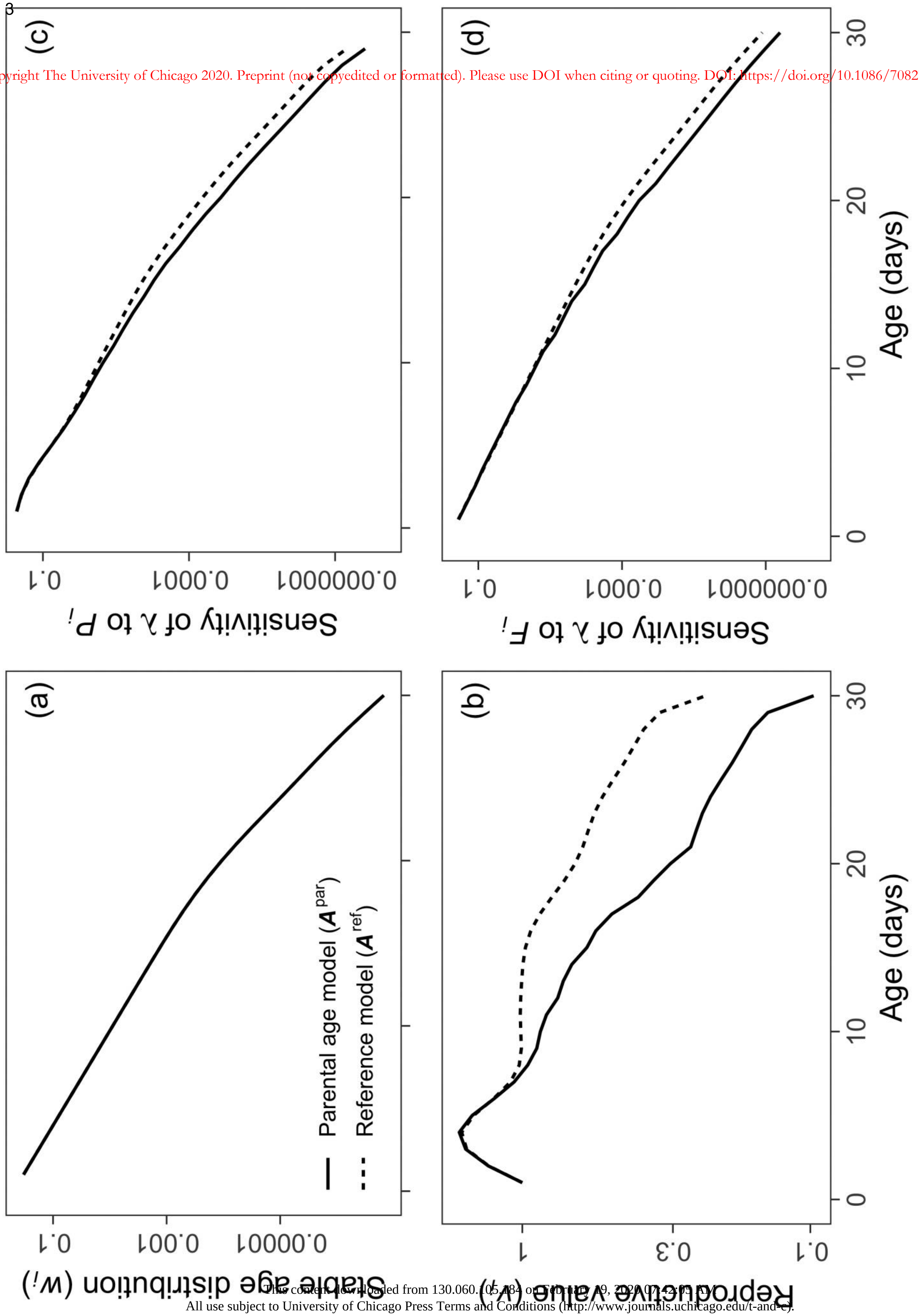
(a)
Stable age distribution (w_i)
0.1
0.001
0.00001
Parental age model ($\boldsymbol{A}^{par}$)
Reference model ($\boldsymbol{A}^{ref}$)
(b)
Reproductive value (v_i)
1
0.3
0.1
0
10
20
30
Age (days)
(c)
Sensitivity of λ to P_i
0.1
0.0001
0.0000001
(d)
Sensitivity of λ to F_i
0.1
0.0001
0.0000001
0
10
20
30
Age (days)

Figure 4

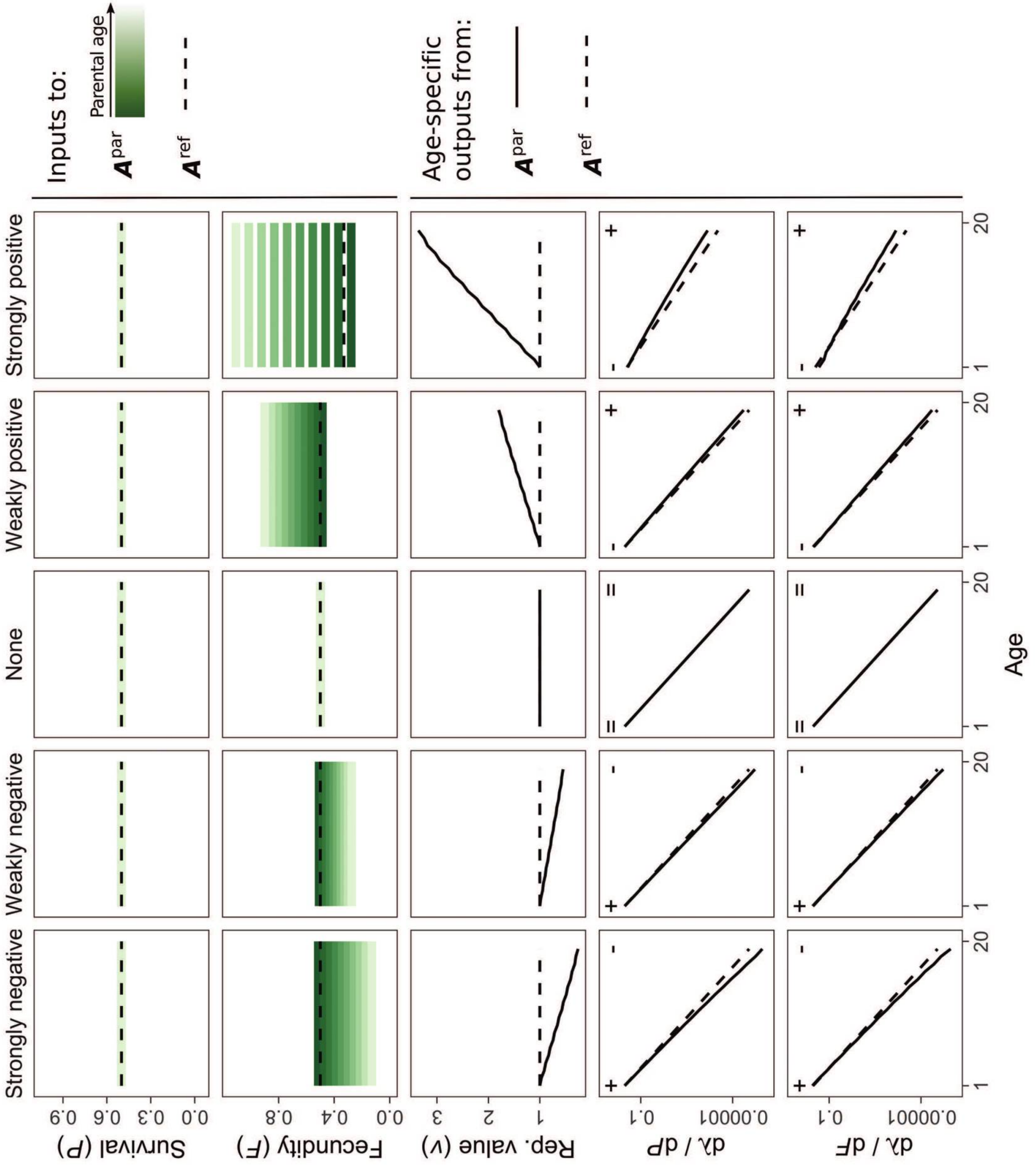
Inputs to:
A^par
Parental age
A^ref
Age-specific outputs from:
A^par
A^ref
Strongly negative
Weakly negative
None
Weakly positive
Strongly positive
Survival (P)
0.0
0.3
0.6
0.9
Fecundity (F)
0.0
0.4
0.8
Rep. value (v)
1
2
3
dλ / dP
0.1
0.00001
dλ / dF
0.1
0.00001
+
-
=
1
20
Age

Figure 5

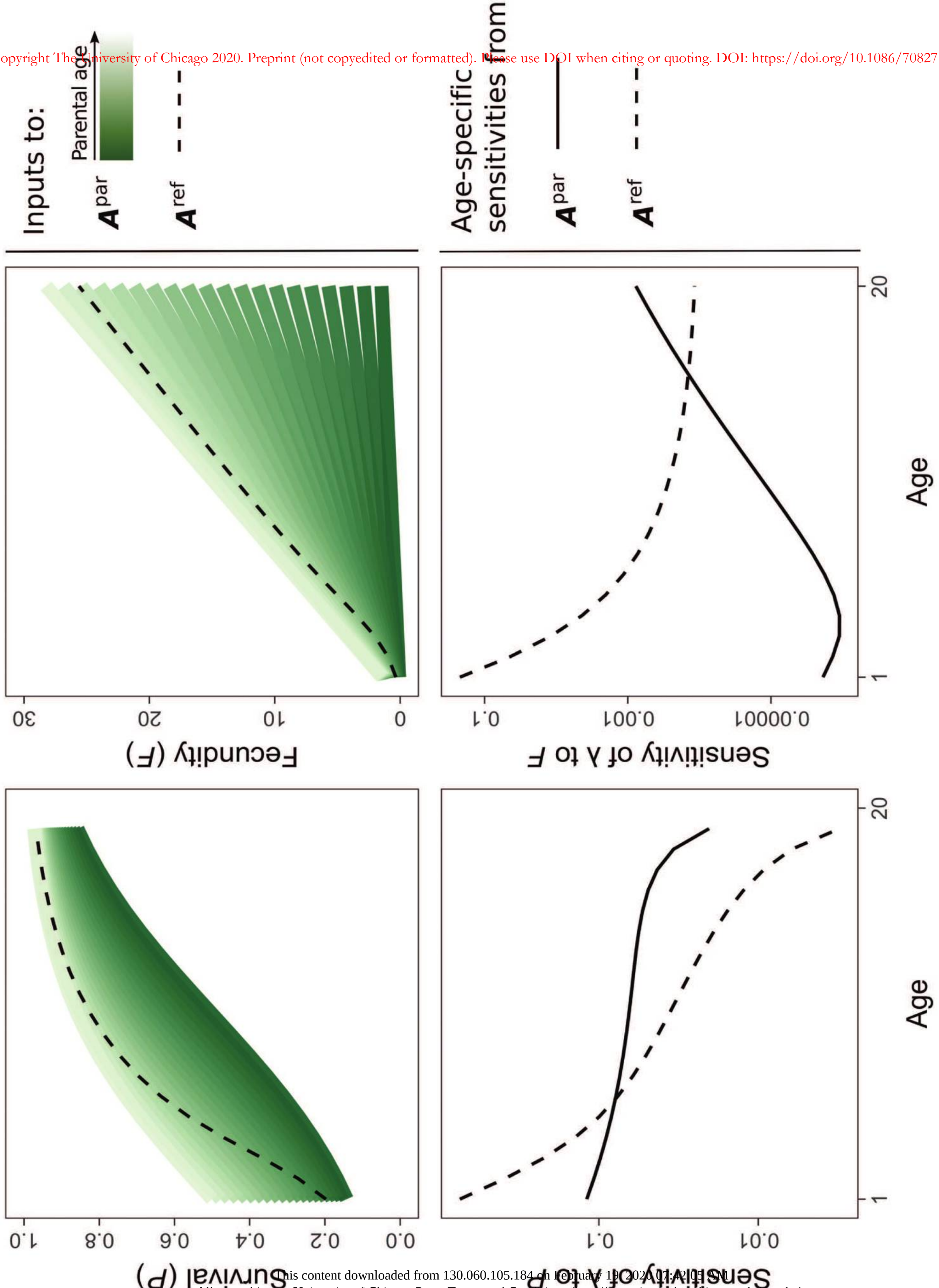
Inputs to:
$\mathbf{A}^{par}$
Parental age
$\mathbf{A}^{ref}$
Age-specific sensitivities from:
$\mathbf{A}^{par}$
$\mathbf{A}^{ref}$
Fecundity (F)
0
10
20
30
Survival (P)
0.0
0.2
0.4
0.6
0.8
1.0
Sensitivity of λ to F
0.1
0.001
0.00001
Sensitivity of λ to P
0.1
0.01
Age
1
20
Age
1
20

Supplementary Material for:

Parental age effects and the evolution of senescence

Patrick M. Barks*, Robert A. Laird

Department of Biological Sciences

University of Lethbridge

Lethbridge, Alberta, T1K 3M4, Canada

*Corresponding author: patrick.barks@gmail.com

Contents

1. Interpretations of parental age effects and offspring quality

We find it rhetorically and conceptually convenient to frame parental age effects as 'age-related declines in offspring quality'. That is, in addition to age-related declines in an individual's probability of survival or rate of reproduction (the two classic fitness components studied in the context of senescence), individuals might also experience age-related declines in the life-long quality of the offspring they produce. The problem with this framing of parental age effects is that 'quality' is ambiguous. If quality is relevant to natural selection, it must presumably relate to rates of survival or reproduction (either of the focal individual or its kin).

Therefore, instead of introducing a third fitness component (offspring quality), we think it is usually technically preferable to frame parental age effects as parental-age-related variation in either of the two classic fitness components — survival and fecundity. Expected rates of survival and fecundity vary with age throughout an individual's lifetime, and age trajectories of survival and fecundity themselves may vary depending on the age of the focal individual's parent when the focal individual was born. Whereas the former framing is parent-focused, the latter framing is population- or genotype-focused. All individuals, at all points in time, have both an age and a parental age, where parental age is a trait that remains fixed throughout an individual's lifetime (see fig. S1).

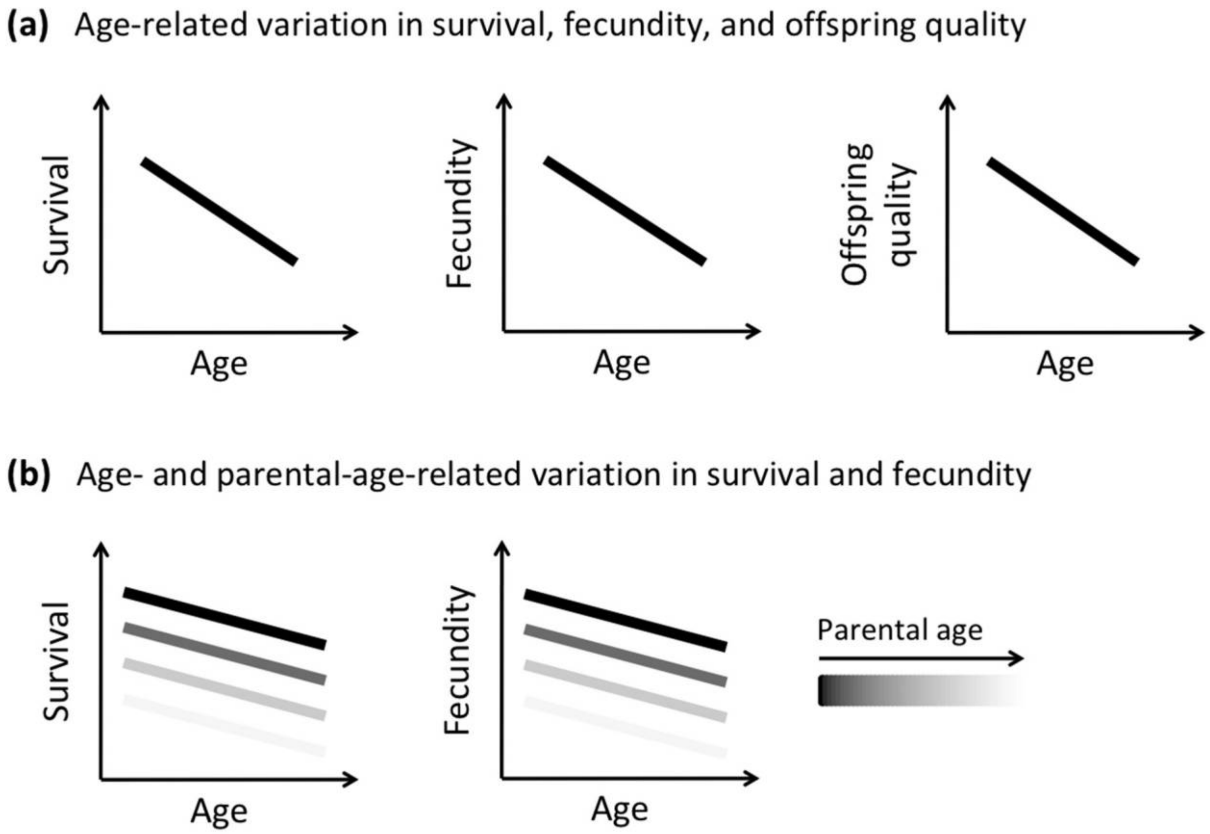

Figure S1: Two conceptual representations of parental age effects. Panel (**a**) depicts age-related variation in three fitness components (survival, fecundity, and offspring quality), whereas panel (**b**) depicts age- *and* parental-age-related variation in the two classic fitness components (survival and fecundity). Parental age is the age of a focal individual's parent when the focal individual was born — a trait that remains fixed throughout life. Whereas framing (**a**) is parent-focused, framing (**b**) is population- or genotype-focused. All individuals, at all points in time, have both an age and a parental age. Framing (**b**) also avoids the ambiguity of the term 'quality', which must somehow relate to survival and fecundity.

2. Background to analysis of matrix projection models

An age-structured population can be projected through time according to

$$\boldsymbol{n}_{t+1} = \boldsymbol{A}\boldsymbol{n}_t,$$

where $\boldsymbol{n}_t$ is a population vector reflecting the number of individuals in each age class i (from 1 through the maximum attainable age class ω) at time t,

$$\boldsymbol{n}_t = \begin{pmatrix} n_1 \\ n_2 \\ \vdots \\ n_\omega \end{pmatrix}_t,$$

and $\boldsymbol{A}$ is a $\omega \times \omega$ projection matrix with per-capita fecundities for each age class across the top row, survival probabilities for age classes 1 through ω–1 on the subdiagonal, and all other elements set to zero,

$$\boldsymbol{A} = \begin{pmatrix} F_1 & F_2 & \cdots & \cdots & F_\omega \\ P_1 & & & & \\ & P_2 & & & \\ & & \ddots & & \\ & & & P_{\omega-1} & \end{pmatrix}.$$

In addition to its application for iterative projection, a number of equilibrium traits can be derived directly from $\boldsymbol{A}$ (Caswell 2001). Specifically, the rate of population increase at equilibrium (λ) is given by the dominant eigenvalue of $\boldsymbol{A}$, and the stable age distribution ($\boldsymbol{w}$) and reproductive value distribution ($\boldsymbol{v}$) are given by the corresponding scaled right and left eigenvectors, respectively. The stable age distribution is scaled to sum to 1, as in

$$\frac{w_i}{\sum_i w_i},$$

and reproductive values are generally scaled such that $v_1 = 1$, as in

$$\frac{v_i}{v_1}.$$

We can also obtain sensitivities to selection from $\boldsymbol{A}$, which represent the change in λ expected to result from a corresponding change in a given matrix element (i.e. an age-specific vital rate). The sensitivity of λ to matrix element $a_{k,l}$ (where k and l are row and column indices, respectively) is given by

$$\frac{\partial\lambda}{\partial a_{k,l}} = \frac{v_k w_l}{\langle \boldsymbol{w}, \boldsymbol{v} \rangle}.$$

3. Constructing $\boldsymbol{A}^{\mathrm{par}}$ with fewer parental age classes than age classes ($s < \omega$)

Recall that an exact correspondence between age classes and parental age classes ($s = \omega$) is convenient, but not necessarily required (either biologically or mathematically). If the number of parental age classes s is strictly less than the number of age classes ω, then at least one parental age class contains more than one age class, in which case we must track the mapping between age classes and parental age classes. For this purpose, we define a vector $\boldsymbol{q}$ of length ω, whose elements q_i are the parental age class j associated with age class i (i.e. the indices reflect age classes and the values reflect parental age classes). For example, in fig. S2 below, $\boldsymbol{q} = \begin{pmatrix} q_1 \\ q_2 \\ q_3 \end{pmatrix} = \begin{pmatrix} 1 \\ 1 \\ 2 \end{pmatrix}$; i.e., offspring of individuals in age classes 1 and 2 have parental age class 1, while offspring of individuals in age class 3 have parental age class 2.

The method for constructing $\boldsymbol{A}^{\mathrm{par}}$ when $s < \omega$ is not fundamentally different than when $s = \omega$; we just need to incorporate the mapping vector $\boldsymbol{q}$. As before, the elements within $\boldsymbol{U}_i$ and $\boldsymbol{M}_i$ are $U_i(k,j)$ and $M_i(k,j)$, respectively, which reflect the probability of a transition from parental age class j to parental age class k, for a given age class i, based on survival and fecundity, respectively. For the $s = \omega$ case we mapped $U_i(k,j)$ to age-by-parental-age specific survival rates ($P_{i,j}$) based on the formula

$$U_i(k,j) = \begin{cases} P_{i,j}, & \text{if } k = j \\ 0, & \text{else} \end{cases}, \qquad [s = \omega]$$

whereas for the $s < \omega$ case the corresponding formula is

$$U_i(k,j) = \begin{cases} P_{i,j}, & \text{if } k = q_i \\ 0, & \text{else} \end{cases}. \qquad [s < \omega]$$

Similarly, for the $s = \omega$ case we mapped $M_i(k,j)$ to age-by-parental-age specific fecundity rates ($F_{i,j}$) based on the formula

$$M_i(k,j) = \begin{cases} F_{i,j}, & \text{if } k = i \\ 0, & \text{else} \end{cases}, \qquad [s = \omega]$$

whereas for the $s < \omega$ case the corresponding formula is

$$M_i(k,j) = \begin{cases} F_{i,j}, & \text{if } k = q_i \\ 0, & \text{else} \end{cases}. \qquad [s < \omega]$$

To clarify, the age class of the parent does not necessarily become the parental age class of the offspring (unless $s = \omega$, in which case age classes and parental age classes correspond exactly). Rather, and more generally, the parental age class that the parent’s exact age falls within becomes the parental age class of the offspring.

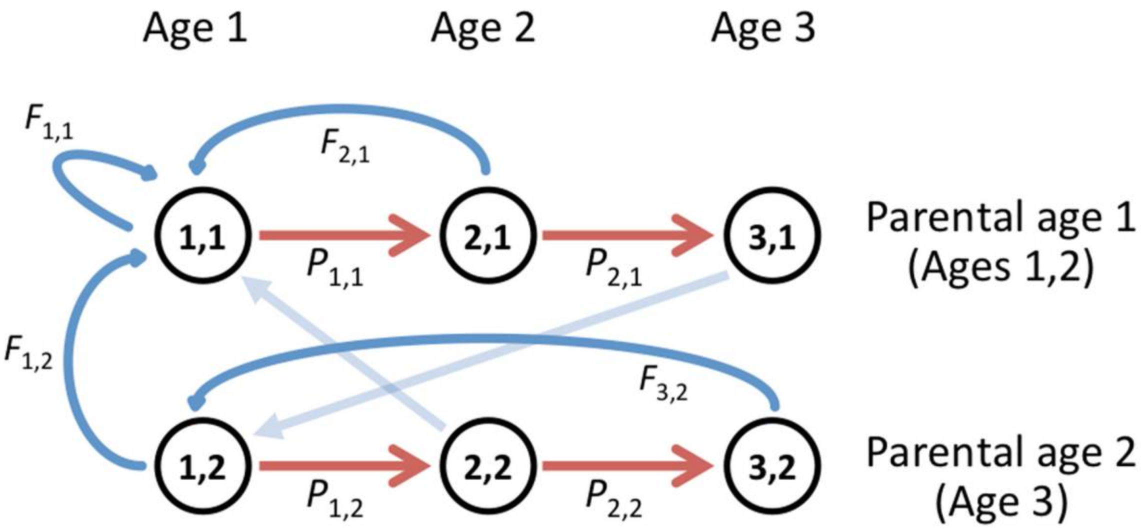

Figure S2: Example life cycle structured by age and parental age, with fewer parental age classes than age classes.

4. Alternative approaches for collapsing $\boldsymbol{A}^{\text{par}}$ to $\boldsymbol{A}^{\text{ref}}$

The method we use to collapse $\boldsymbol{A}^{\text{par}}$ to $\boldsymbol{A}^{\text{ref}}$ — averaging across parental age classes weighted by the stable distribution — is not the only possible way of creating a reference matrix. We could have instead taken an arithmetic average of transition rates across parental age classes, or taken an average weighted by the reproductive value distribution instead of the stable distribution. However, in our experience, these alternative approaches do not preserve *any* equilibrium characteristics (not λ, nor the relative stable age distribution, reproductive value distribution, or sensitivities), in which case potential differences in selection trajectories between $\boldsymbol{A}^{\text{par}}$ and $\boldsymbol{A}^{\text{ref}}$ could not necessarily be attributed directly to the parental age effect. It is in fact possible to collapse a matrix such that λ, the stable distribution, reproductive value distribution, and elasticities of λ are all preserved (see the 'genealogical collapsing' method of Bienvenu et al. 2017), but the interpretation of such a model would differ from our desired framework (e.g. the collapsed population vector would no longer be in units of 'individuals', and collapsed survival transitions may have values exceeding 1).

A secondary advantage of our collapsing method is that the resulting $\boldsymbol{A}^{\text{ref}}$ corresponds to the projection matrix that we would expect to estimate from the population of interest if we were simply ignorant about the parental age effect. That is, if our population of interest were subject to parental age effects but we didn't realize it, and simply constructed an age-based projection model with transition rates estimated separately for each age class, the transition rates we would estimate would effectively be an average across parental age classes weighted by the relative distribution of parental age classes within age classes (assuming random sampling).

5. Census methodology for *Lemna minor* data from Barks and Laird (2015)

The *Lemna minor* data used in the current study are from Barks and Laird (2014, 2015). In that study, survival and fecundity were documented on a daily basis for all of the 542 ramet offspring that detached from 41 parental fronds. Because there is no simple instantaneous marker of frond death in *L. minor*, death was defined as the census following the release of a frond’s final offspring, meaning that reproduction is not conditional on survival per se.

Lemna minor exhibits birth-flow rather than birth-pulse reproduction (sensu Caswell 2001, Section 4.2) in that offspring may detach from their parents continuously throughout the projection or census interval. Because our method of deriving transition rates involves smoothing, our transition rates do not exactly map to a specific census type (birth-flow, birth-pulse pre-breeding, or birth-pulse post-breeding). The raw data entering our generalized additive models correspond to counts from a post-breeding birth-pulse census design, in that our age index i starts at 0 rather than 1, e.g.

$$P_1 = \frac{l_1}{l_0},$$

where l_i is the proportion of the cohort surviving to age i, and $l_0 = 1$. However, the smoothed transition rates output from our models (described in the following section) correspond more closely to a birth-flow census design, where the transition rates represent estimates for the midpoint of each age interval, e.g.

$$P_1 \approx \frac{1}{2}\left(\frac{l_1}{l_0} + \frac{l_2}{l_1}\right).$$

6. Estimation of age-by-parental-age transition rates for *Lemna minor*

Because empirical age-by-parental-age transition rates for *Lemna minor* were noisy (fig. S3), we elected to parameterize $\boldsymbol{A}^{\mathrm{par}}$ with smoothed transition rates obtained from generalized additive models, fit using the *gam* function in the R package mgcv (Wood 2011). Separately for each vital rate, we fit and compared six different models, using a binomial error distribution for the survival models and a Poisson error distribution for the fecundity models. Each model included a thin-plate regression spline smoother for age (with default penalty parameters), but models varied in their specification of the group-level parental age effect (these specifications were based on Pedersen et al. 2019):

1. no parental age effect
2. random intercepts for parental age groups
3. smoother for parental age groups: common shape and wiggliness
4. smoother for parental age groups: common shape, independent wiggliness
5. smoother for parental age groups: independent shape, common wiggliness
6. smoother for parental age groups: independent shape and wiggliness

Models 1 and 3-6 correspond to models G, GS, S, GI, and I in Pedersen et al. (2019). Model 2 includes a smoother for age and traditional random intercept for parental age group. We compared model fits using AIC, and used predicted transition rates from the single best model for all subsequent analyses.

The best model with respect to survival was #5 (smoother for parental age groups with independent shape and common wiggliness; fig. S4), and with respect to fecundity was #3 (smoother for parental age groups with common shape and wiggliness; fig: S5).

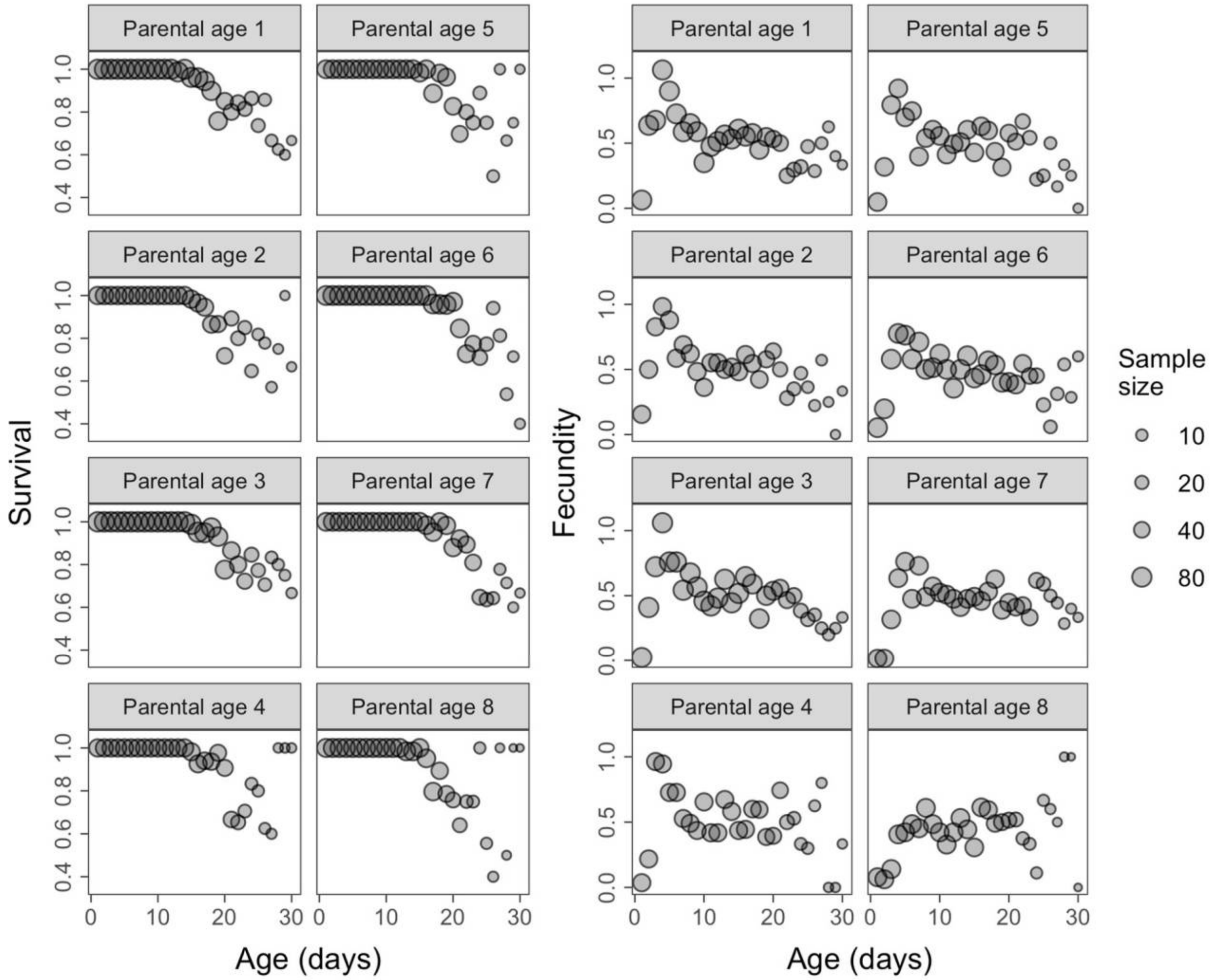

Figure S3: Empirical age-by-parental-age-specific transition rates in *Lemna minor*. The thirty possible parental ages were split into eight parental age groups of similar sample size, as explained in the main text. Point area is proportional to the number of plants from which each transition rate was estimated. Note that the two leftmost columns depict daily survival probabilities rather than survivorship, and so values do not necessarily decline monotonically with age.

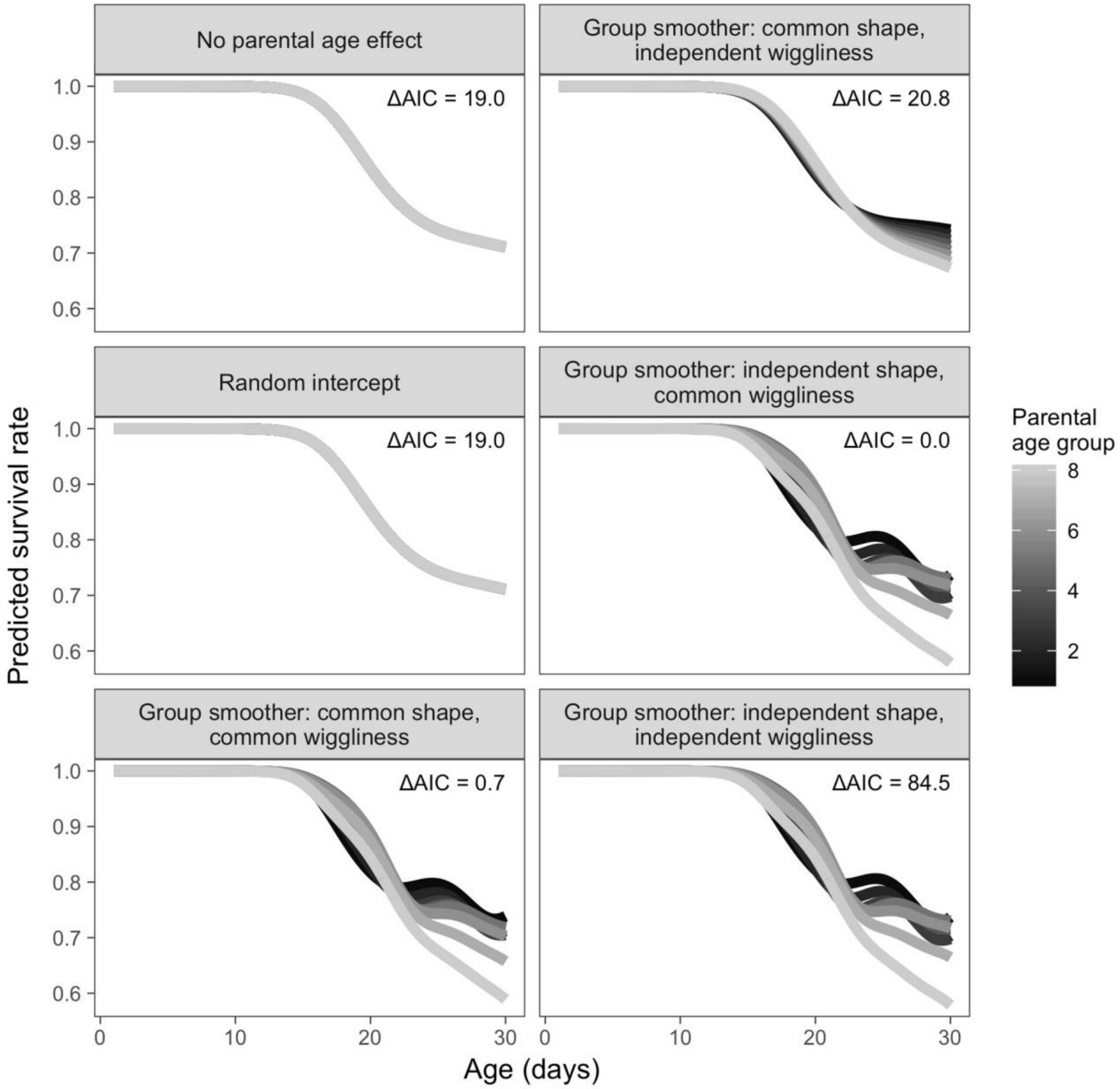

Figure S4: Predicted age-by-parental-age survival rates in *Lemna minor*, based on generalized additive models reflecting six different specifications of the group-level parental age effect, as described in Section 6 above.

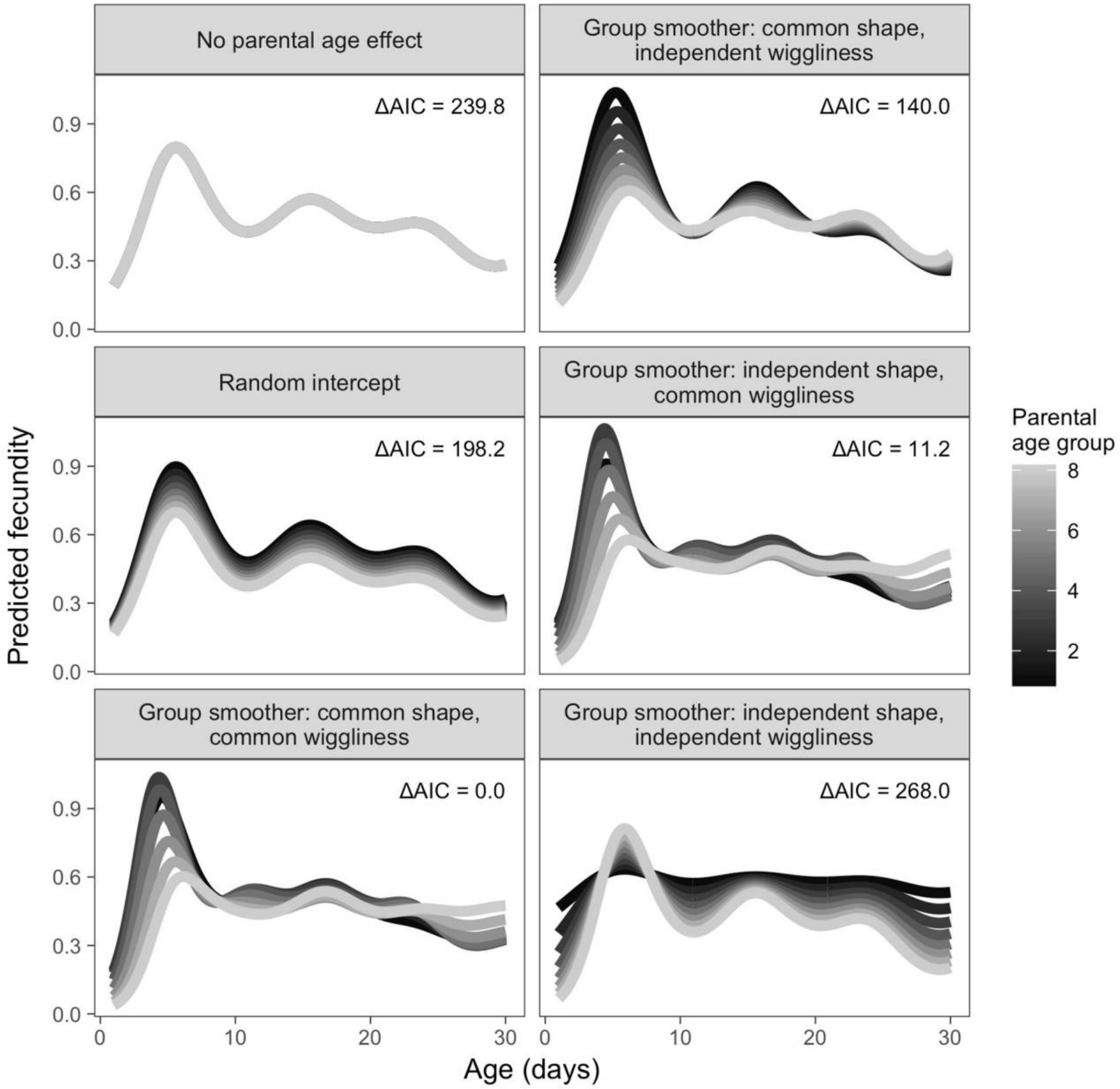

Figure S5: Predicted age-by-parental-age rates of fecundity in *Lemna minor*, based on generalized additive models reflecting six different specifications of the group-level parental age effect, as described in Section 6 above.

7. Method for constructing simulated life cycles

To assess the generality of the model results from *L. minor*, we also applied the parental age model to simulated life cycles spanning a continuum of parental age effects, from strongly negative to strongly positive. In all cases we set the number of age classes to $\omega = 20$ and the number of parental age classes to $s = 10$. We generated population-level transition rates in three steps:

1. Create baseline age-trajectories of survival (P_i) and fecundity (F_i)
2. Add parental age structure to the baseline trajectories to generate $P_{i,j}$ and $F_{i,j}$
3. Add a constant to all fecundity transitions $F_{i,j}$ to achieve the desired value of λ for $\boldsymbol{A}^{\text{par}}$

1. Create baseline age-trajectories of survival (P_i) and fecundity (F_i)

We generated baseline age-trajectories of survival (P_i) and fecundity (F_i) using an age-independent value of 0.5 for survival and 1 for fecundity (see fig. S6).

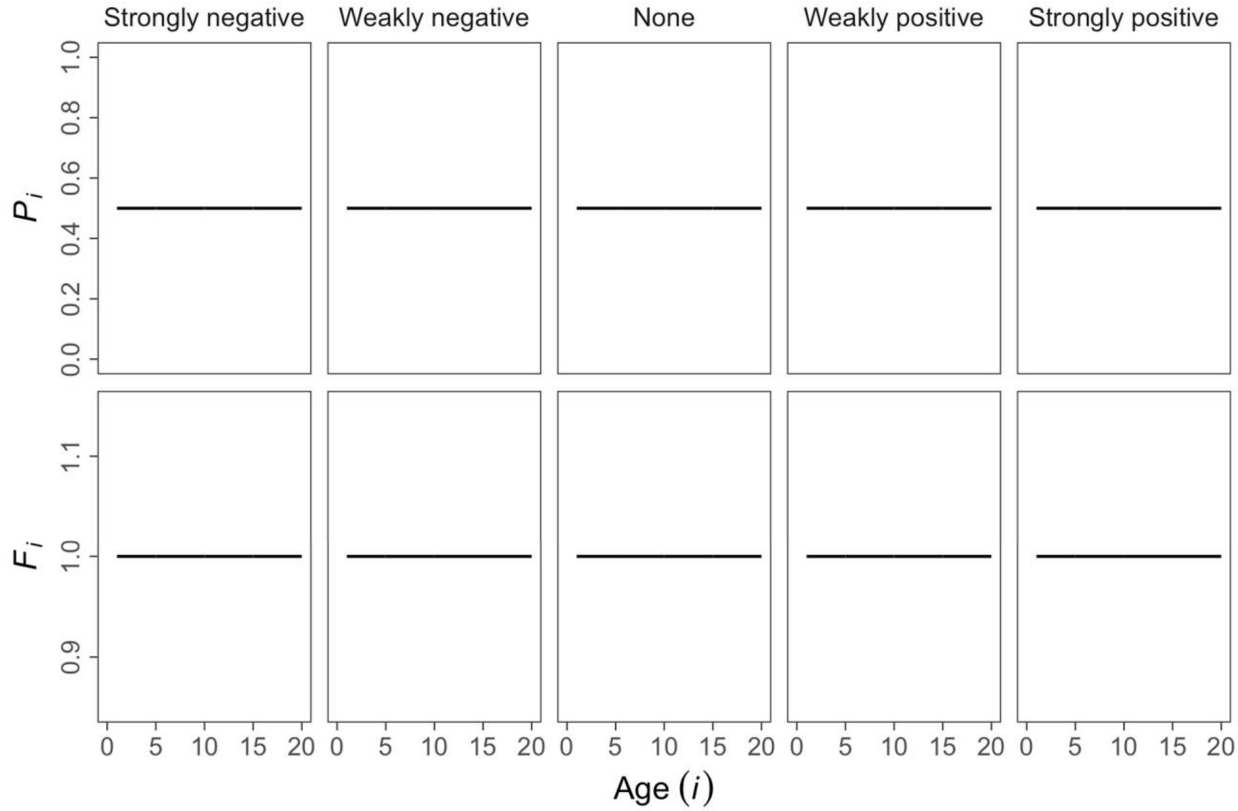

Figure S6: Baseline age trajectories of survival (P_i) and fecundity (F_i) used to generate the simulated life cycles, based on step 1 above. The simulated life cycles will eventually reflect a continuum of parental age effects, from strongly negative to strongly positive.

2. Add parental age structure to the baseline trajectories to generate $P_{i,j}$ and $F_{i,j}$

We generated parental age effects on fecundity (fig. S7) by multiplying age-specific fecundity values (i.e. the baseline values described above) with a parental-age-dependent constant, with constants equally spaced over a pre-defined range. For the strongly negative parental age effect, constants ranged from 1.6 (for *j* = 1, the youngest parental age class) to 0.4 (for *j* = 10, the oldest parental age class),

$$F_{i,j} = \eta_j F_i,$$

$$\{\eta_1, \eta_2, \eta_3, \dots, \eta_{10}\} = \{1.60, 1.4\overline{6}, 1.3\overline{3}, \dots, 0.40\}.$$

For the strongly positive parental age effect we simply reversed the sequence above, as in

$$\{\eta_1, \eta_2, \eta_3, \dots, \eta_{10}\} = \{0.40, 0.5\overline{3}, 0.6\overline{6}, \dots, 1.60\}.$$

For the weakly negative parental age effect we used a sequence between 1.3 and 0.7, as in

$$\{\eta_1, \eta_2, \eta_3, \dots, \eta_{10}\} = \{1.30, 1.2\overline{3}, 1.1\overline{6}, \dots, 0.70\},$$

which we again reversed to generate the weakly positive parental age effect, as in

$$\{\eta_1, \eta_2, \eta_3, \dots, \eta_{10}\} = \{0.70, 0.7\overline{6}, 0.8\overline{3}, \dots, 1.30\}.$$

In the main text, we did not explore a parental age effect on survival, so age-by-parental-age specific survival values ($P_{i,j}$) were simply set to the age-specific baseline,

$$P_{i,j} = 0.5.$$

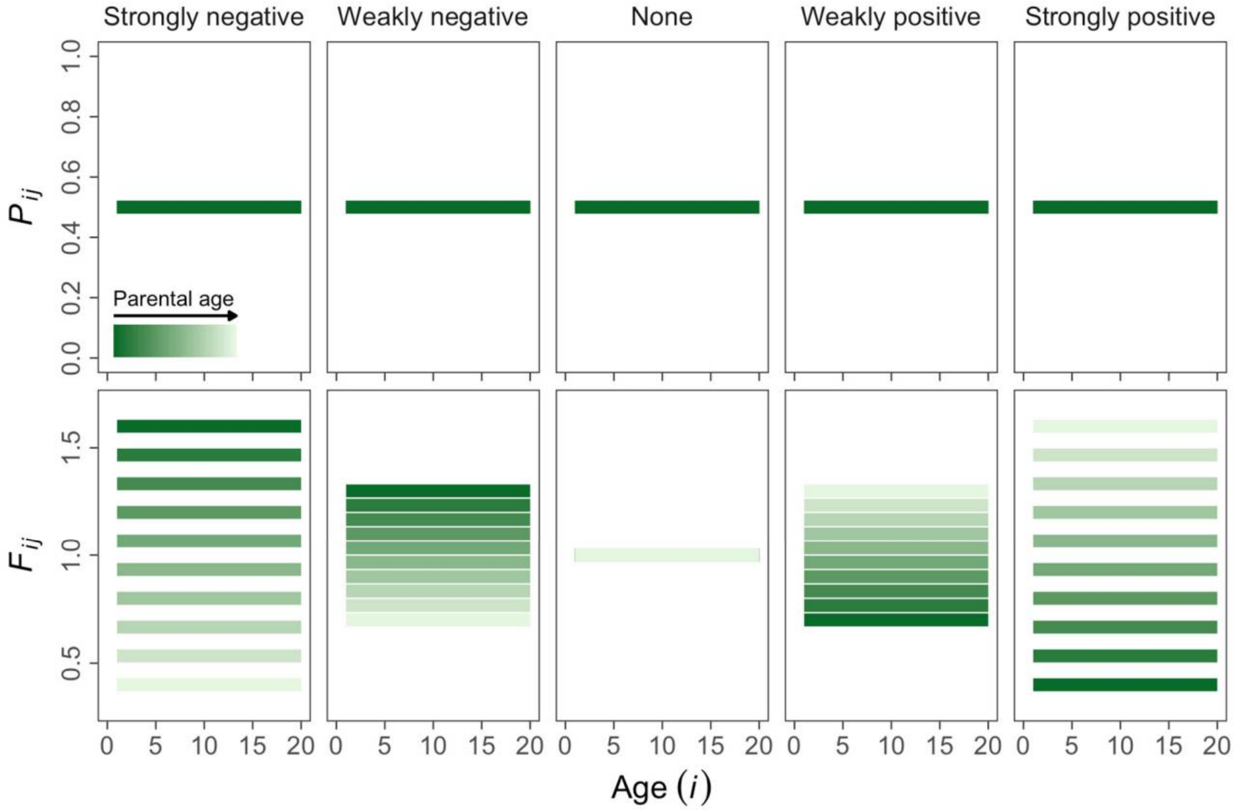

Figure S7: Baseline age-by-parental-age trajectories of survival ($P_{i,j}$) and fecundity ($F_{i,j}$) for simulated life cycles spanning a range of parental age effects, based on step 2 above.

3. Add a constant to all fecundity transitions $F_{i,j}$ to achieve the desired value of λ for $\boldsymbol{A}^{\text{par}}$

Our final step was to adjust the fecundity transition rates to achieve a pre-designated value for the population growth rate of $\boldsymbol{A}^{\text{par}}$ ($\lambda = 1$ in the main text). For a given life cycle we adjusted all fecundity transition rates by a common multiplicative constant τ, as in

$$\tau F_{i,j},$$

with the value of τ determined through numerical optimization using the *optim* function in R (see fig. S8).

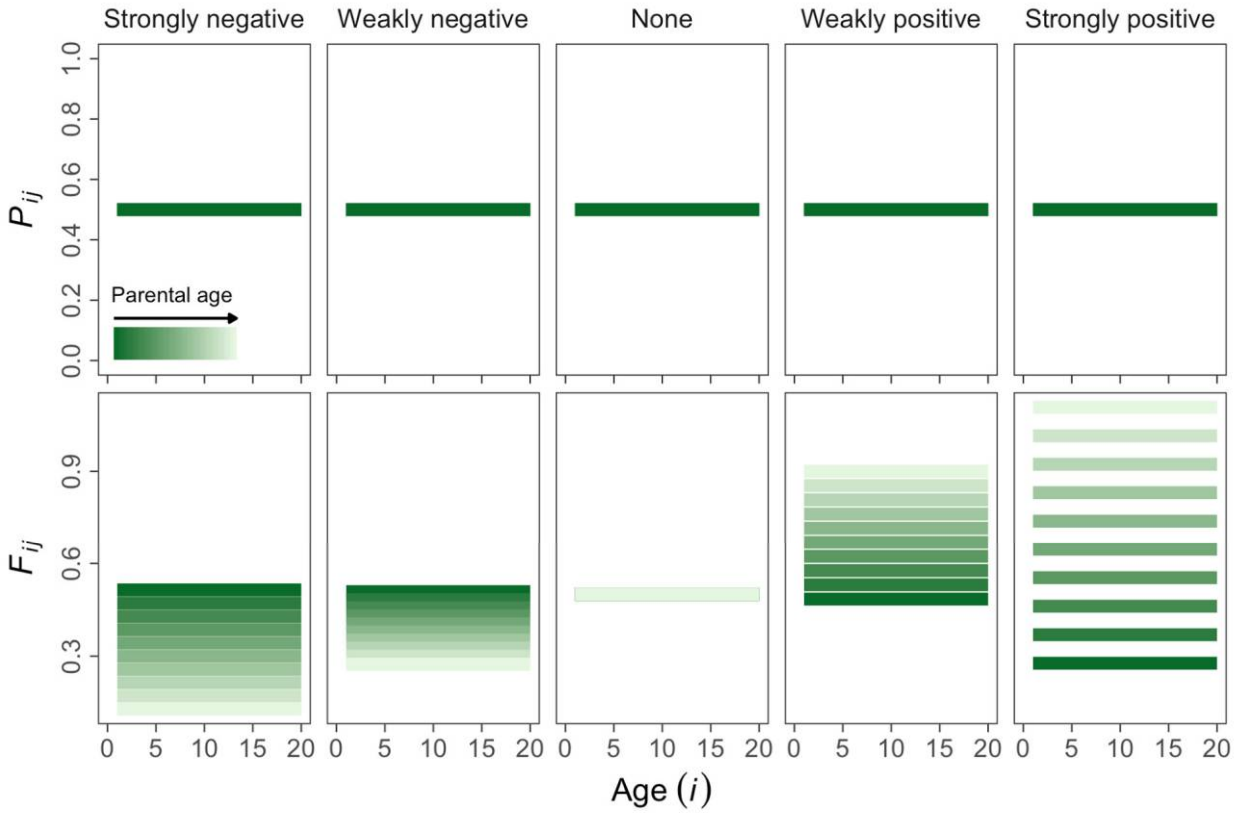

Figure S8: Final age-by-parental-age trajectories of survival ($P_{i,j}$) and fecundity ($F_{i,j}$) for simulated life cycles spanning a range of parental age effects, following step 3 above. Each set of transition rates yields a population growth rate of $\lambda = 1$. Note that the values depicted here correspond to the top two rows of fig. 4 in the main text.

8. Sensitivity analyses

Here we explore some alternative parameterizations of $\boldsymbol{A}^{\text{par}}$, to ensure that our main results are robust. Specifically, we repeat the analyses described above with each the following changes, in turn:

a) vary the population growth rate of $\boldsymbol{A}^{\text{par}}$
b) generate a parental age effect on survival rather than fecundity

a) Vary the population growth rate of $\boldsymbol{A}^{\text{par}}$

In our main analyses, we set the population growth rate of $\boldsymbol{A}^{\text{par}}$ to $\lambda = 1$. Here we explore a range of λ values, from 0.6 to 1.4. We use the life cycle with the strongly negative parental age effect (described in Section 6 above) as our baseline, again adjusting the fecundity transition rates up or down to achieve the desired λ.

The results for this scenario were qualitatively similar to our main analyses (fig. S9): regardless of λ, relative reproductive values and sensitivities of λ to survival and fecundity declined more strongly with age in $\boldsymbol{A}^{\text{par}}$ compared to $\boldsymbol{A}^{\text{ref}}$ (i.e. accounting for negative parental age effects led to a steeper age-related decline in the force of selection).

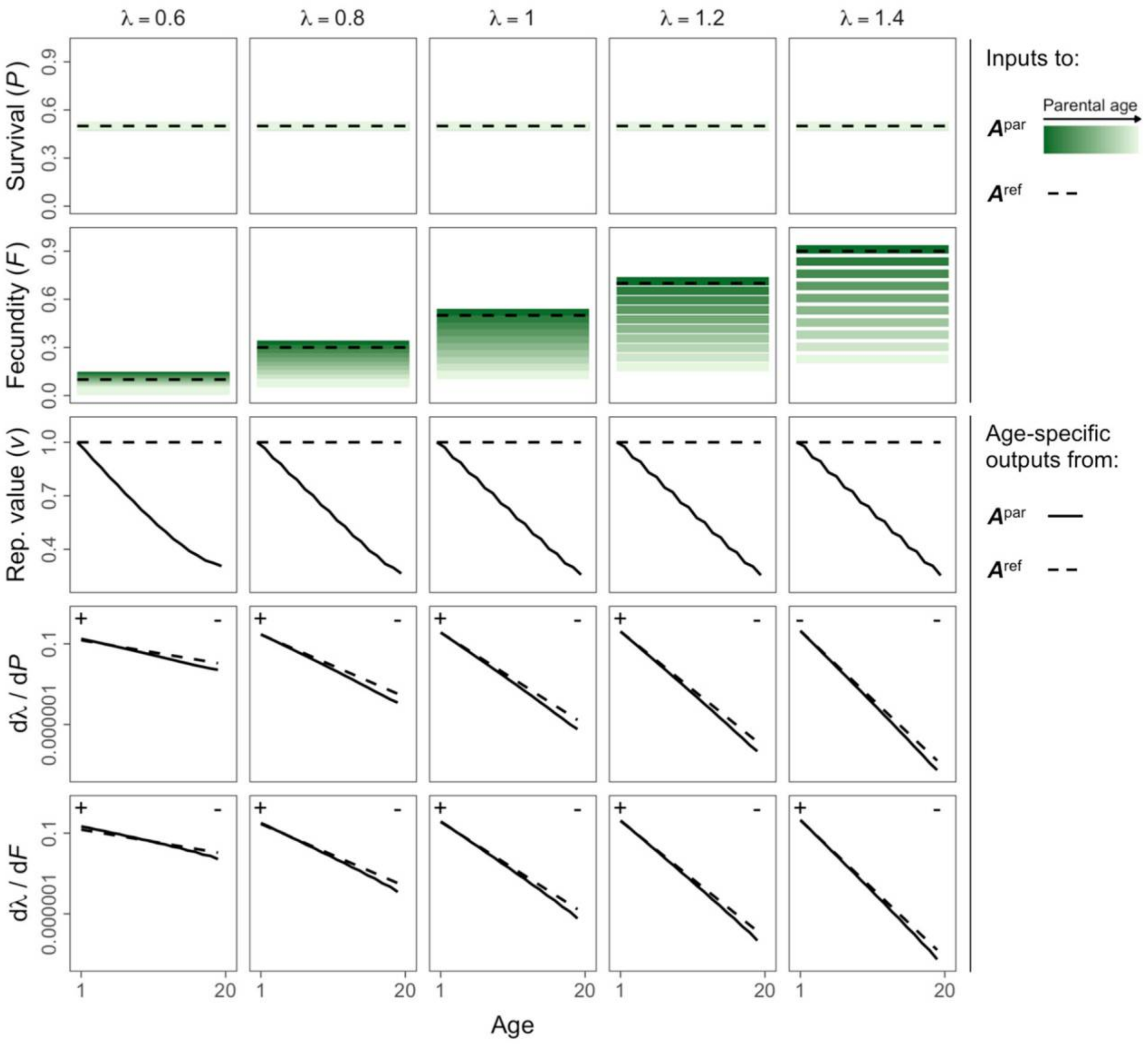

Figure S9: Model inputs and age-specific outputs with respect to five simulated life cycles spanning a range of population growth rates, from strongly declining ($\lambda = 0.6$) to strongly increasing ($\lambda = 1.4$). Each life cycle exhibits a negative parental age effect on fecundity. The top two rows show transition rate inputs to the respective models (model $\boldsymbol{A}^{\text{par}}$ accounts for parental age effects whereas $\boldsymbol{A}^{\text{ref}}$ does not), whereas the bottom three rows depict age-specific model outputs: relative reproductive values (as defined in the main text), sensitivities of λ to survival ($\mathrm{d}\lambda/\mathrm{d}P$), and sensitivities of λ to fecundity ($\mathrm{d}\lambda/\mathrm{d}F$). Symbols at the top of some panels indicate, for the youngest or oldest age classes, whether the value from $\boldsymbol{A}^{\text{par}}$ is greater than (+) or less than (−) the corresponding value from $\boldsymbol{A}^{\text{ref}}$.

b) Parental age effect on survival rather than fecundity

In our main analyses we examined a parental age effect on offspring fecundity. Here we examine a parental age effect on offspring survival.

We used the same basic parameterization as described in Section 6, except that we generated the parental age effect by adding a parental-age-dependent constant to logit-transformed age-specific survival values (i.e. the baseline values described above), with constants equally spaced over a pre-defined range. For the strongly negative parental age effect, constants ranged from +0.5 (for *j* = 1, the youngest parental age class) to –0.5 (for *j* = 10, the oldest parental age class),

$$P_{i,j} = \text{inverse\_logit}(\eta_j + \text{logit}(P_i)),$$

$$\{\eta_1, \eta_2, \eta_3, \dots, \eta_{10}\} = \{0.50, 0.3\overline{8}, 0.2\overline{7}, \dots, -0.50\}.$$

For the strongly positive parental age effect we simply reversed the sequence above, as in

$$\{\eta_1, \eta_2, \eta_3, \dots, \eta_{10}\} = \{-0.50, -0.3\overline{8}, -0.2\overline{7}, \dots, 0.50\}.$$

For the weakly negative parental age effect we used a sequence between +0.25 and –0.25, as in

$$\{\eta_1, \eta_2, \eta_3, \dots, \eta_{10}\} = \{0.250, 0.19\overline{4}, 0.13\overline{8}, \dots, -0.250\},$$

which we again reversed to generate the weakly positive parental age effect, as in

$$\{\eta_1, \eta_2, \eta_3, \dots, \eta_{10}\} = \{-0.250, -0.19\overline{4}, -0.13\overline{8}, \dots, 0.250\}.$$

Age-by-parental-age specific fecundity values ($F_{i,j}$) were simply set to the age-specific baseline values,

$$F_{i,j} = F_i,$$

which were subsequently adjusted to achieve a population growth rate of $\lambda = 1$.

The results for this scenario (fig. S10) were qualitatively similar to our main analyses: negative parental age effects reduced the relative value of late-life reproduction and led to slightly steeper age-related declines in sensitivities of λ to survival and fecundity than were predicted by the reference model. In contrast, positive parental age effects increased the relative value of late-life reproduction, leading to slightly shallower age-related declines in sensitivities of λ to survival and fecundity.

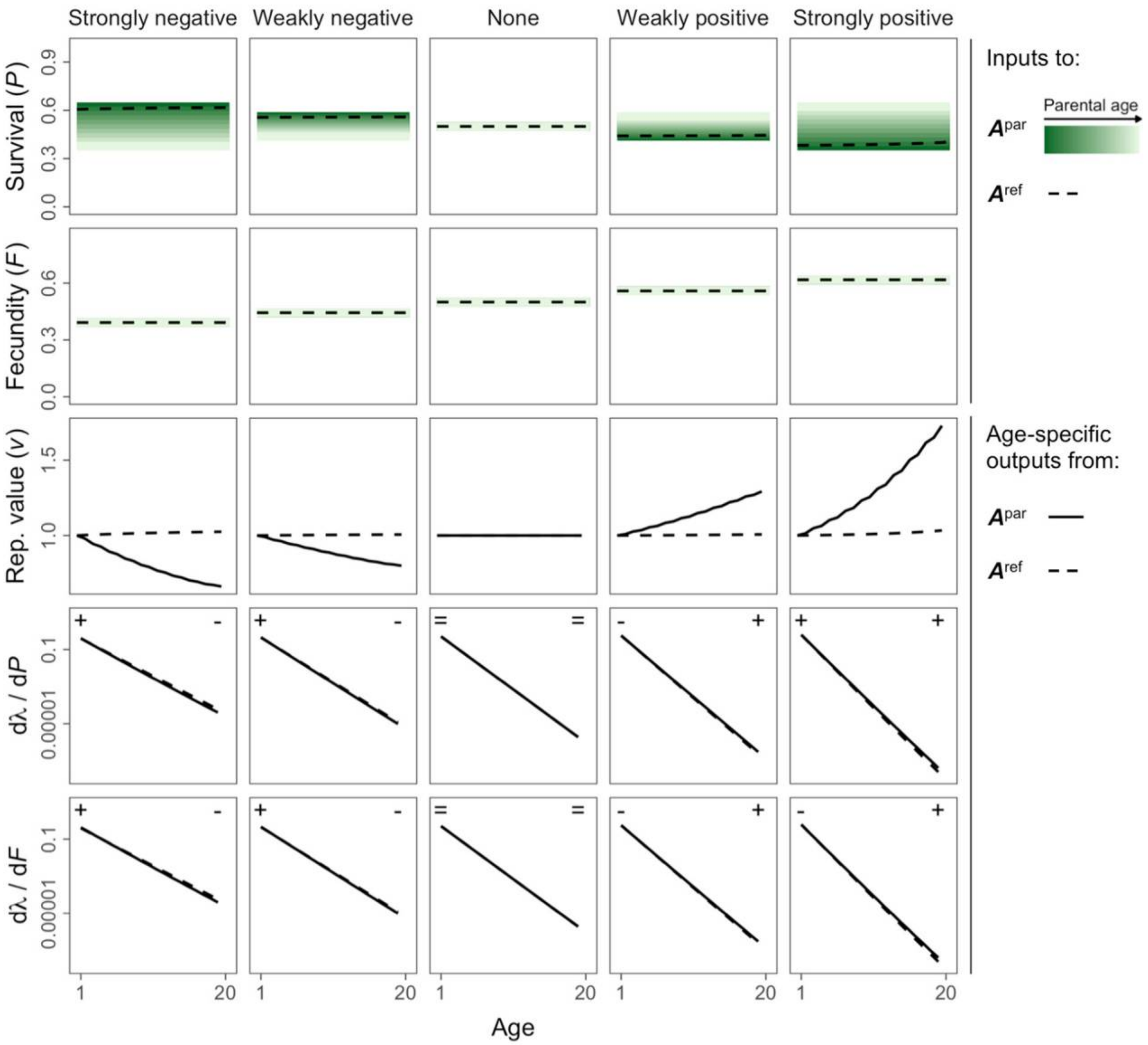

Figure S10: Model inputs and age-specific outputs with respect to five simulated life cycles spanning a continuum of parental age effects on survival, from strongly negative (leftmost column) to strongly positive (rightmost column). The top two rows show transition rate inputs to the respective models (model $\boldsymbol{A}^{\text{par}}$ accounts for parental age effects whereas $\boldsymbol{A}^{\text{ref}}$ does not), whereas the bottom three rows depict age-specific model outputs: relative reproductive values (as defined in the main text), sensitivities of λ to survival ($\mathrm{d}\lambda/\mathrm{d}P$), and sensitivities of λ to fecundity ($\mathrm{d}\lambda/\mathrm{d}F$). Symbols in the bottom two rows indicate, for the youngest or oldest age classes, whether the value from $\boldsymbol{A}^{\text{par}}$ is greater than (+), less than (–), or equal to (=) the corresponding value from $\boldsymbol{A}^{\text{ref}}$.

References

Barks, P. M., and R. A. Laird. 2014. Data from: Senescence in duckweed: age-related declines in survival, reproduction, and offspring quality. Dryad Digital Repository. https://doi.org/10.5061/dryad.t938n

Barks, P. M., and R. A. Laird. 2015. Senescence in duckweed: age-related declines in survival, reproduction and offspring quality. Functional Ecology 29:540–548.

Bienvenu, F., E. Akcay, S. Legendre, and D. M. McCandlish. 2017. The genealogical decomposition of a matrix population model with applications to the aggregation of stages. Theoretical Population Biology 115:69–80.

Caswell, H. 2001. *Matrix population models: construction, analysis, and interpretation, 2nd ed*. Sinauer, Sunderland, MA.

Pedersen, E. J., D. L. Miller, G. L. Simpson, and N. Ross. 2019. Hierarchical generalized additive models in ecology: an introduction with mgcv. PeerJ 7:e6876.

Wood, S. N. 2011. Fast stable restricted maximum likelihood and marginal likelihood estimation of semiparametric generalized linear models. Journal of the Royal Statistical Society: Series B 73:3–36.